AD-A052 612 FLORIDA INST OF TECH MELBOURNE F/G 9/5
RESONATOR EFFECTS IN MICROWAVE CASSEGRAIN ANTENNAS.(U)
1975 W E CLAASSEN

UNCLASSIFIED NL

| OF |
AD
A052 612

END
DATE
FILMED
5-78
DDC

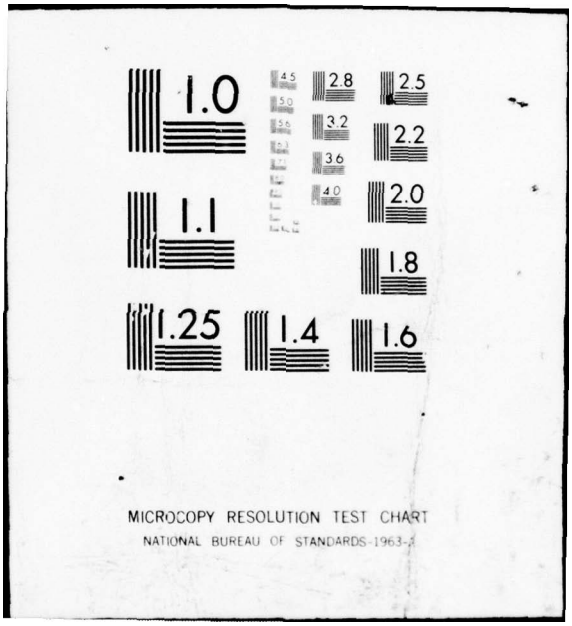
1.0
1.1
1.25
1.4
1.6
1.8
2.0
2.2
2.5
2.8
3.2
3.6
4.0
4.5
5.0
5.6
MICROCOPY RESOLUTION TEST CHART
NATIONAL BUREAU OF STANDARDS-1963-A

(6) RESONATOR EFFECTS IN MICROWAVE CASSEGRAIN ANTENNAS.

(2)

by

(10) Walter E. Claassen, Jr.

B.S., United States Military Academy, 1961

(9) Master's thesis,

Submitted to the Graduate Faculty

in partial fulfillment of

the requirements for the degree of

Master of Science

in

Electrical Engineering

Florida Institute of Technology

(12) 95 p. (11) 1975

(Signature)

ABSTRACT

The effects of standing waves in the region between the feed horn and subdish of a Cassegrain antenna are examined experimentally. Evaluation of the experimental results indicate the existence of a resonator in this region which makes calibration of the Cassegrain antenna necessary in order to determine the influence of the resonator on a signal which is transmitted or received. It has been established that the radiation pattern characteristics are profoundly influenced by the location of the feed horn with respect to the parabolic (main) reflector. These two effects (the horn-subdish resonator effect and the primary feed pattern alteration caused by the main reflector) are judged to be the dominant factors influencing the observed on-axis oscillations occuring with changes in the feed horn-subdish spacing. The influence of multipath has been examined and so far as can be determined by this study is not a contributing factor. Further research is recommended; a) using a dipole probe to measure the standing waves in the horn-subdish region, b) applying a leveled frequency sweeping technique, and c) development of an error curve to be used in antenna calibration.

ACKNOWLEDGEMENTS

The suggestions and encouragement of my thesis advisor and chairman of the thesis committee, Dr. Walter M. Nunn, Jr. are gratefully acknowledged. In addition, I would like to express my appreciation to the Commanding Officer of Patrick Air Force Base and his staff for the use of facilities for part of the experimental work for this thesis, and to the Athletic Director, Mr. Arthur K. Loche, for the use of the Gynmasium for experimental purposes. Special appreciation must be given to my wife, Betty, and my children for their understanding and support during my academic endeavors.

TABLE OF CONTENTS

LIST OF SYMBOLS

Symbol	Description	Units	Page*
a	One half the transverse axis of a hyperbola	cm	6
A_e	Effective aperture of an antenna	cm^2	65
A_{eh}	Effective aperture of the feed horn	cm^2	11
b	One half the conjugate axis of a hyperbola	cm	6
B	Blockage		18
B_m	Beam area		65
c	Velocity of light in free space (2.997×10^{10})	cm/sec	70
D	Directivity		65
D_e	Diameter of the equivalent parabola	cm	9
D_m	Diameter of the main dish	cm	3
D_m/λ_d	Diameter of main dish in wavelengths		19
D_s	Diameter of the subdish	cm	3
e	Eccentricity of the hyperbola		6
E_D	Electric field strength of direct wave	v/m	38
E_R	Electric field strength of reflected wave	v/m	38

*Page where symbol first appears.

Symbol	Description	Units	Page
f	Frequency	Hz	
f_d	Design frequency	Hz	19
f_{new}	Low frequency of spatial filter bandwidth	Hz	70
f'_{new}	High frequency of spatial filter bandwidth	Hz	70
f_o	Frequency of the wave in free space	Hz	68
F	Focal point of the main dish and one focus of subdish		5
F'	Second focus of subdish		5
F_c	Distance between the foci	cm	3
F_e	Focal length of equivalent parabola	cm	8
F_m	Axial distance between the main dish and its focus (focal length)	cm	3
F/D	Focal length to diameter ratio		10
F_e/D_m	F/D ratio of system		10
F_m/D_m	F/D ratio of main dish		10
G	Antenna gain	db	38
G_B	Gain losses due to blockage	db	19
G_o	Gain as a function of directivity		65
k	Constant related to antenna efficiency		65
L_r	Distance between F' and the face of the subdish	cm	8

Symbol	Description	Units	Page
L_v	Distance between F and the face of the subdish	cm	3
M	Magnification		11
P_D	Power of the direct wave	watts	38
P_R	Power of the reflected wave	watts	38
r_D	Path length of direct wave	cm	38
r_R	Path length of reflected wave	cm	38
R_c	Fresnel-Fraunhofer Boundary of the Cassegrain antenna	m	49
x_e	Horizontal distance between F and the point of the surface of the equivalent parabola	cm	8
x_m	Horizontal distance between F and any point on the main dish	cm	5
x_s	Horizontal distance between F and any point on the subdish	cm	6
y_e	Vertical coordinate which corresponds to x_e	cm	8
y_m	Vertical coordinate which corresponds to x_m	cm	5
y_s	Vertical coordinate which corresponds to x_s	cm	6
α	Subdish half angle, measured from F'	degrees	3
β	Grazing angle of a reflected wave	degrees	39
θ	Main dish half angle measured from F	degrees	3

Symbol	Description	Units	Page
λ	Wavelength	cm	18
λ_d	Design wavelength	cm	19
λ_{new}	Wavelength of f_{new}	cm	70
λ'_{new}	Wavelength of f'_{new}	cm	70
λ_o	Wavelength in free space	cm	70
ϕ_1	Vertical beam width	degrees	65
ψ_1	Horizontal beam width	degrees	65

LIST OF ILLUSTRATIONS

LIST OF TABLES

CHAPTER I. INTRODUCTION

A. Purpose of Investigation

This thesis was suggested by an indication of the existence of standing waves in the region between the feed horn and the subdish of a Cassegrain antenna. The purpose of this study was to experimentally examine the influence of these standing waves upon the radiation pattern and the general characteristics of microwave Cassegrain antennas.

The existence of standing waves in the space between the feed horn and the subdish of a Cassegrain antenna was apparently first observed in 1973 by Bushko[1]*, an undergraduate student at the Florida Institute of Technology. Although the established ray tracing design and analysis techniques associated with Cassegrain antennas will not account for standing waves in the antenna system, these waves are derivable from electromagnetic theory.

The presence of standing waves in the spatial interval between the feed horn and the subdish has been experimentally confirmed by measurements performed in the study reported herein. These two system components form a resonator which

---

*Parenthetical numerals placed superior to the line of text refer to the References.

resembles the Fabry-Perot resonator in optics. The observed resonator behavior, which arises whenever two reflecting surfaces are brought into axial alignment within the vicinity of one another, results in the antenna system exhibiting a "Microwave Transfer Function" comparable to the "Optical Transfer Function"[2] well known in the optical field. This microwave transfer function posseses an "amplitude response" (which in optics is called the "modulation transfer function" for a lens), and a "phase response" (in optics, the "phase transfer function" for a lens). A Cassegrain antenna, operating over a given frequency range must be "calibrated" over this range (e.g., by precise measurement) so as to properly "correct" the signal arriving at the detector to account for the influence of the antenna. Experimental investigations also reveal that the radiation pattern of the antenna is strongly influenced by the observed resonator effects which points to the necessity for a more refined mathematical analysis to predict the antenna performance than has heretofore been employed.

B. Background

The Cassegrain antenna, named for the French Physician and inventor of the optical telescope from which it was derived, is designed by applying ray optics techniques used in the design of this high magnification telescope. Since the classic paper by Hannan[3] introducing the technique in microwave antenna design, geometric optics[4,5] and scalar diffraction theory[6,7] have emerged as the standard design and analysis procedures for Cassegrain antennas. The relevant geometry is shown in Fig. 1.1. An important relationship for the parabolic main dish is given by:

$$\tan\left(\frac{\theta}{2}\right)=\frac{1}{4}\left(\frac{D_m}{F_m}\right) \tag{1.1}$$

For the hyperbolic subdish, the relationships are:

$$\frac{1}{\tan\theta}+\frac{1}{\tan\alpha}=2\left(\frac{F_c}{D_s}\right), \quad \text{and} \tag{1.2}$$

$$1-\frac{\sin\frac{1}{2}(\theta-\alpha)}{\sin\frac{1}{2}(\theta+\alpha)}=2\left(\frac{L_v}{F_c}\right). \tag{1.3}$$

The diameter of the main dish (D_m), the focal length of the main dish (F_m), the distance between the foci of the hyperbolic subdish (F_c) and the main dish half angle (θ) are usually determined by consideration of antenna performance and

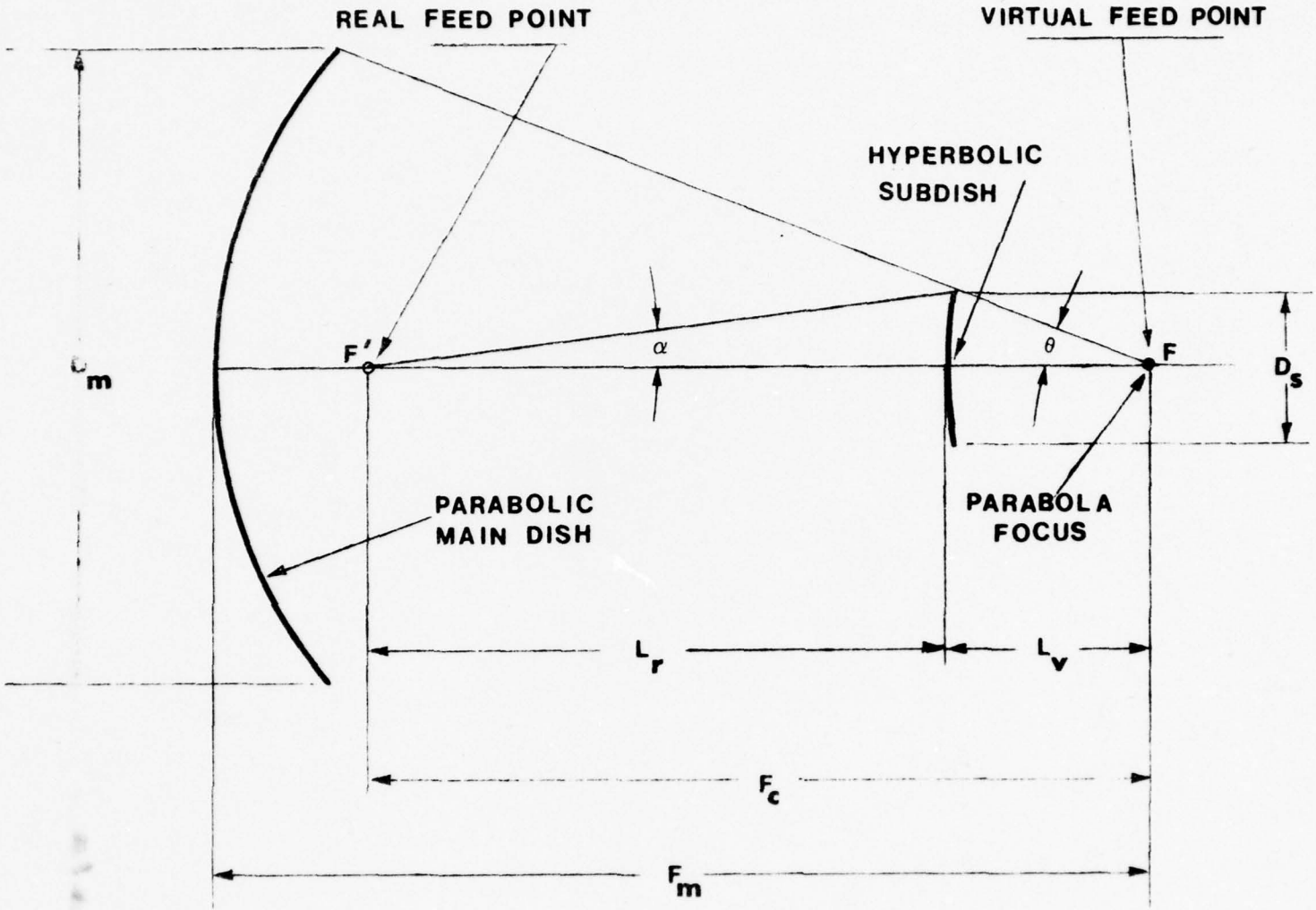

Fig. 1.1. Geometry of the Cassegrain Antenna.

space limitations and become the four known parameters[3]. These quantities are then used to calculate the diameter of the subdish (D_s), the subdish half angle (α) and the distance between the face of the subdish and the focus of the main dish along the axis (L_v), which also provides the distance between the face of the subdish, and the other focus of the subdish (L_r). For the present antenna, D_m, F_m and θ were fixed by the available equipment, and D_s was judiciously selected, and the remaining parameters were calculated.

Hannan[3] refers to the real focal point (F'), and the virtual focal point (F). This terminology tends to be confusing since the virtual focal point is actually the focal point of the parabolic main dish and one of the foci of the hyperbolic subdish, while the actual focal point is the other focus of the hyperbolic subdish as well as the location of the feed. For this reason, the terms real feed point (F') and virtual feed point (F) will be used in this study. The contour of the main dish is given by the simple parabolic equation:

$$x_m = \frac{y_m^2}{4F_m} \quad , \tag{1.4}$$

where x_m is the horizontal distance (in cm) from the virtual feed point (F) to any point of the surface, and y_m is the

corresponding vertical distance to the same point (in cm). The hyperbolic subdish contour is found from the relation:

$$x_s = a\left[\sqrt{1+(y_s/b)^2} - 1\right], \tag{1.5}$$

where a and b are given by:

$$a = \frac{F_c}{2e}, \tag{1.6}$$

$$b = a\sqrt{e^2-1}, \tag{1.7}$$

and the eccentricity e by:

$$e = \frac{\sin \frac{1}{2}(\theta+\alpha)}{\sin \frac{1}{2}(\theta-\alpha)}. \tag{1.8}$$

The parameters a, b and e are commonly used in geometry[8] to describe a hyperbola: a is one half the transverse axis, b is one half the conjugate axis, and e is the eccentricity.

Examination of Fig. 1.1 illustrates a simplified process of ray tracing from the real focal point (F') to the subdish, along the line describing the half angle α, and reflection from the subdish to the main dish along the line described by the half angle Θ. The ray then reflects from the main dish parallel to the axis. The geometry of the system is such that the ray would appear to be originating at the virtual feed point (F) of the system. That is, the subdish is de-

signed by making the eccentricity of the hyperbolic surface dependent on both α and Θ, as shown in Eq.(1.8), so that the focus of the parabolic main dish and one of the foci of the hyperbolic subdish are coincident (F); consequently, the angle of reflection of a ray originating at the other focus of the subdish (F'), is such that the path may be traced through the virtual feed point (F). The fundamental geometric property of a parabola which applies to parabolic reflector antennas is that a line from the focal point of a parabola to a point on the surface is equal to the distance between the point and the directrix of the parabola. Kraus[9] has shown that this principle, applied to reflector antennas, results in a constant distance for any path from the focal point to the surface of a parabola plus the path from the point on the surface to the aperture of the parabola. Since the total path length is constant, all waves from an isotropic source at the focus reflected from the parabola will arrive at the aperture in phase. Extension of the ray tracing idea described leads to the conclusion that the system may be reduced to a single reflector antenna with the feed located at the virtual feed point (F) of the main dish. This concept is suitable for a qualitative analysis of the system, but is not in general useful for an accurate quantitative analysis[3].

Hannan describes a useful equivalent antenna which is graphically derived by combining the hyperbola and the parabola into an equivalent parabola as shown in Fig. 1.2. The equivalent antenna is a parabola with the focal point at the real feed point (F') of the Cassegrain antenna. Although the equivalent parabola (shown dotted in Fig. 1.2) faces in the opposite direction from that of the original antenna, this does not invalidate the analysis. While other configurations may be represented by equivalent surfaces, the equivalent parabola is unique to the Cassegrain geometry, and is the result of ray tracing approximations[3]. The most important relationships between the equivalent parabola and the parameters of the actual system are:

$$\frac{1}{4}\left(\frac{D_m}{F_e}\right) = \tan(\alpha/2) \ , \tag{1.9}$$

$$x_e = \frac{y_e^2}{4F_e} \ , \tag{1.10}$$

$$\frac{F_e}{F_m} = \frac{\tan(\theta/2)}{\tan(\alpha/2)} = \frac{L_v}{L_r} \ , \quad \text{and} \tag{1.11}$$

$$e = \frac{L_r + L_v}{L_r - L_v} \ . \tag{1.12}$$

Equations (1.9), (1.11) and (1.12) define the equivalent parabola in terms of the original system, while Eq.(1.10) is the

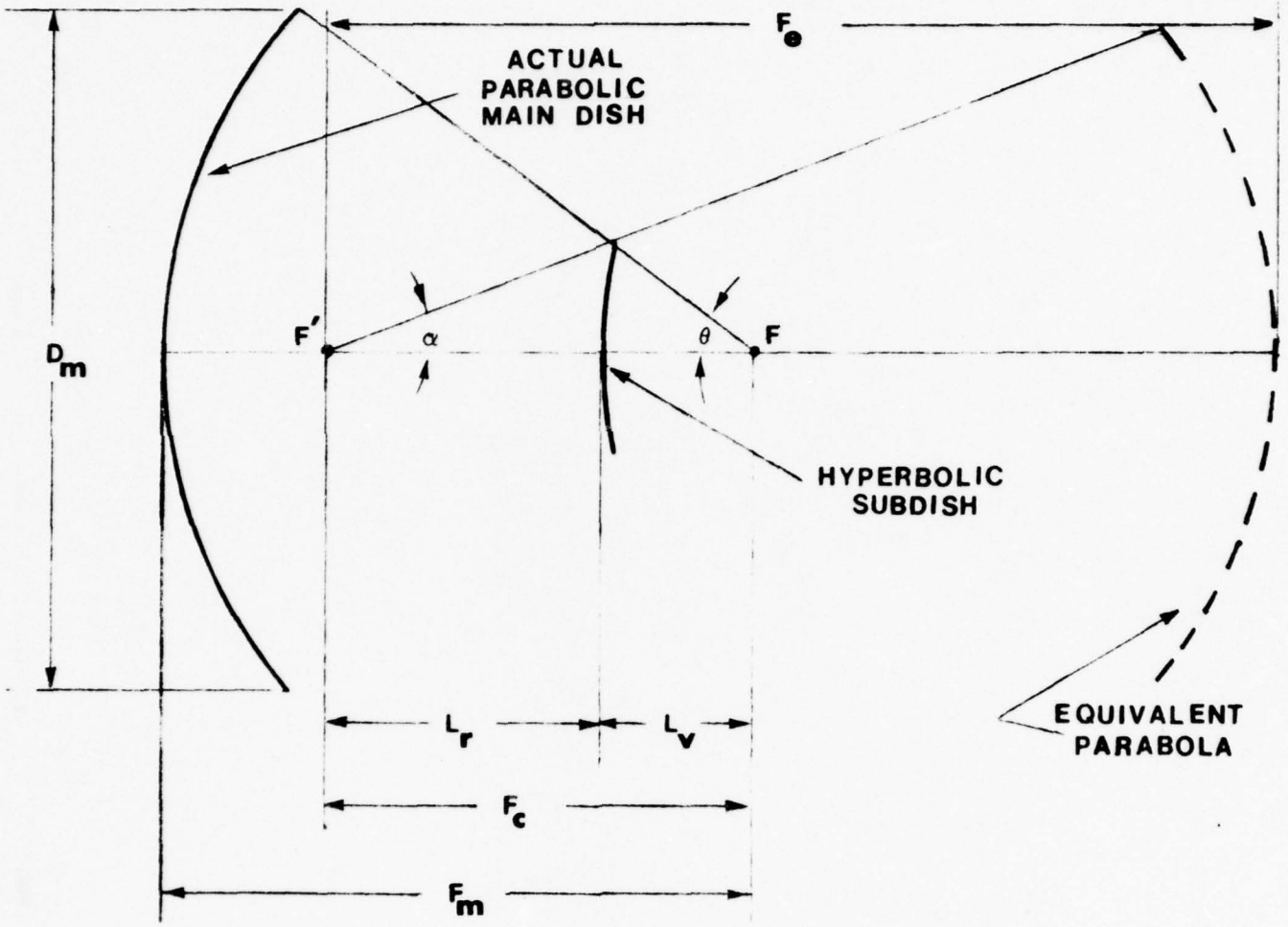

Fig. 1.2. Equivalent Parabola Concept.

expression for the equivalent parabola itself. Two parameters which become more important in evaluating the antenna design are obtained from the equivalent parabola, the F/D ratio and magnification.

The selection of an appropriate F/D ratio for a parabolic reflector antenna becomes complicated, since it requires consideration of several conflicting factors[10]. In order to reduce "spillover" of the parabolic reflector, a small F/D ratio (approximately 0.25) is desirable, while a large F/D ratio (≥ 1.0) produces an antenna with a desirable low signal-to-noise ratio[4]. As the F/D ratio increases, however, the physical length of the system increases, which presents mechanical problems such as supporting structures for the feed systems and the need for larger and more expensive radomes[10].

Jensen[4] gives an acceptable range for F_m/D_m in a Cassegrain antenna from 0.25 to 0.42. For a Cassegrain antenna, the equivalent parabola focal length is also used to describe the system properties, and is given by F_e/D_m. For the antenna used in this study, the value is 1.7681, indicative of a low noise system, while the physical F_m/D_m ratio is 0.3704, indicating low spillover and low side lobe levels.

Spillover is the energy lost to the reflector surface. In a Cassegrain antenna, there are two types of spillover to

consider; forward spillover, which is the energy radiating past the subdish, and rearward spillover, which is the energy reflected by the subdish that radiates past the main dish. Forward spillover contributes directly to the side lobe level of the Cassegrain antenna radiation pattern, as will be demonstrated in Chapter III[3,4,5].

The ratio of the effective aperture of the feed (A_{eh}) to the physical aperture of the feed is the magnification (M) of the antenna. The convex shape of the subdish allows the use of a smaller feed than would be required to properly illuminate the equivalent parabola with a feed horn located at the focal point of the main dish (F). Although this effect is analogous to the magnifying properties of an optical telescope, it must not be confused with the magnification of an optical telescope with an eyepiece, in which the term applies to the relative sizes of the image and the object. The magnification of a Cassegrain antenna is given by[3]:

$$M = \frac{F_e}{F_m} \tag{1.13}$$

The basic geometry described by Hannan[3] was used by Jensen[4] and Henry[5] to formalize design procedures for the Cassegrain antenna. Their important contributions will be utilized in the design procedures presented in Chapter II for

the antenna under investigation.

The results of careful experimental measurements conducted in the microwave frequency range near 10 GHz, and in the optical range using a helium-neon laser, which confirm the accuracy of the design procedure and the significance of the Microwave Transfer Function of the Cassegrain antenna are presented in Chapter III. These results point to the necessity of carefully calibrating a microwave Cassegrain antenna in order to properly interpret the spectral characteristics of a signal received from such an antenna. In addition, these results emphasize the importance of more refined analytical techniques in the study of Cassegrain antennas than have heretofore been employed.

CHAPTER II. ANTENNA DESIGN

A. Available Components

The Electrical Engineering Department had all of the components of a Cassegrain antenna on hand. These included an Andrew Corporation Model 18775 reflector 121.92 cm in diameter, a flared feed horn with a rectangular aperture (39.42 cm^2), a subdish 16.51 cm in diameter and a system of three struts and ancillary hardware for mounting the subdish. The large reflector, which was to be used as a main dish, is mounted on a rigid frame work on a heavy triangular base which is fitted with casters. The dish is attached to the frame in such manner as to allow vertical scan from 83^o to 97^o from the horizontal, while insuring against slippage from the desired position. The weight of the base assures stability, while the casters allow lateral movement of the antenna.

B. The Parabolic Main Dish

Although to all appearances and belief, the Andrew Model 18775 Reflector was parabolic in shape, it was checked in detail, since variation from the paraboloid would result in an invalid design. The Andrew Corporation was queried concern-

ing the design specifications of the reflector, since information on the Model 18775 is not available in current catalogs. Since no response could be obtained from the manufacturer, it became necessary to determine the shape of the reflector by measurement.

The reflector was set in position with its aperture perpendicular to the floor, as verified by careful measurement with a precision angle measuring level; and a plumb bob was hung from the top dead center of the dish by a strong cord which had been wet and stretched to dry, and marked at one inch intervals. Measurements were then taken at each mark to the surface of the dish, and the data recorded. This method served to verify the diameter of the dish at 48 inches (121.92 cm). The data collected in this manner was adjusted to be usable in Eq.(1.4) by subtracting each horizontal measurement from 8 inches (greatest depth of dish) and taking vertical measurements from the center of the dish. The data from two arbitrary points were selected, and used to compute and confirm the focal length of the dish (45.16 cm). The horizontal distance (x_m) was then calculated for each of the data points, and the results compared to the measured data, confirming the parabolic shape, and the following values:

$$D_m = 121.92 \text{ cm, and} \qquad F_m = 45.16 \text{ cm.} \tag{2.1}$$

The half angle Θ is then found using Eq.(1.1):

$$\theta = 68.04^\circ \tag{2.2}$$

C. Blockage

The remainder of the design procedure is more complicated than that of the main dish. The size of the subdish and the feed horn, together with their respective locations, determine the degree of aperture blockage. Hannan[3] introduced the concept of aperture blockage, and pointed out that, although blockage is not a serious problem in Cassegrain telescopes because of the short wavelength of light, it has been the principal limitation of Cassegrain microwave antennas. The presence of the subdish creates a "hole" in the center of the radiation path which causes reduced gain and increased side lobes, both of which are undesirable in a microwave antenna system. Jensen[4] and Henry[5] have extended and simplified the approximations made by Hannan[3] to reduce the effects of blockage in the early stages of antenna design. The method used by Hannan to find minimum blockage lends itself to analysis of an antenna system, but is difficult to

employ for antenna design. Figure 2.1 illustrates the minimum blockage condition.

Since a ray reflecting from the subdish appears to be originating at the focal point of the parabola, or the virtual feed point, reference to Fig. 2.1 shows that the feed horn casts a "shadow" on the main dish. That is, the feed horn blocks some rays from arriving at the main dish. The subdish also blocks some of the rays which are reflected from the main dish from radiating out of the system. The degree of blockage, then, is a function of the position of the feed horn as well as the size of the subdish. If the feed horn is placed all the way back against the main dish, its location would no longer cause a blockage problem, but, now, the subdish does not fully intercept the feed horn fields, resulting in forward spillover. On the other hand, if the feed horn is moved too close to the subdish, it casts a large shadow, and becomes the dominant blockage factor. The feed horn aperture size in wavelengths determines the beamwidth and, in turn, the angle which must be subtended to illuminate the subdish. Therefore, the location of the feed horn determines the size and shape of the subdish, as well as influencing the subdish location. The location of the subdish is also a function of the F_m/D_m ratio of the main dish[5]. The foregoing inter-dependence

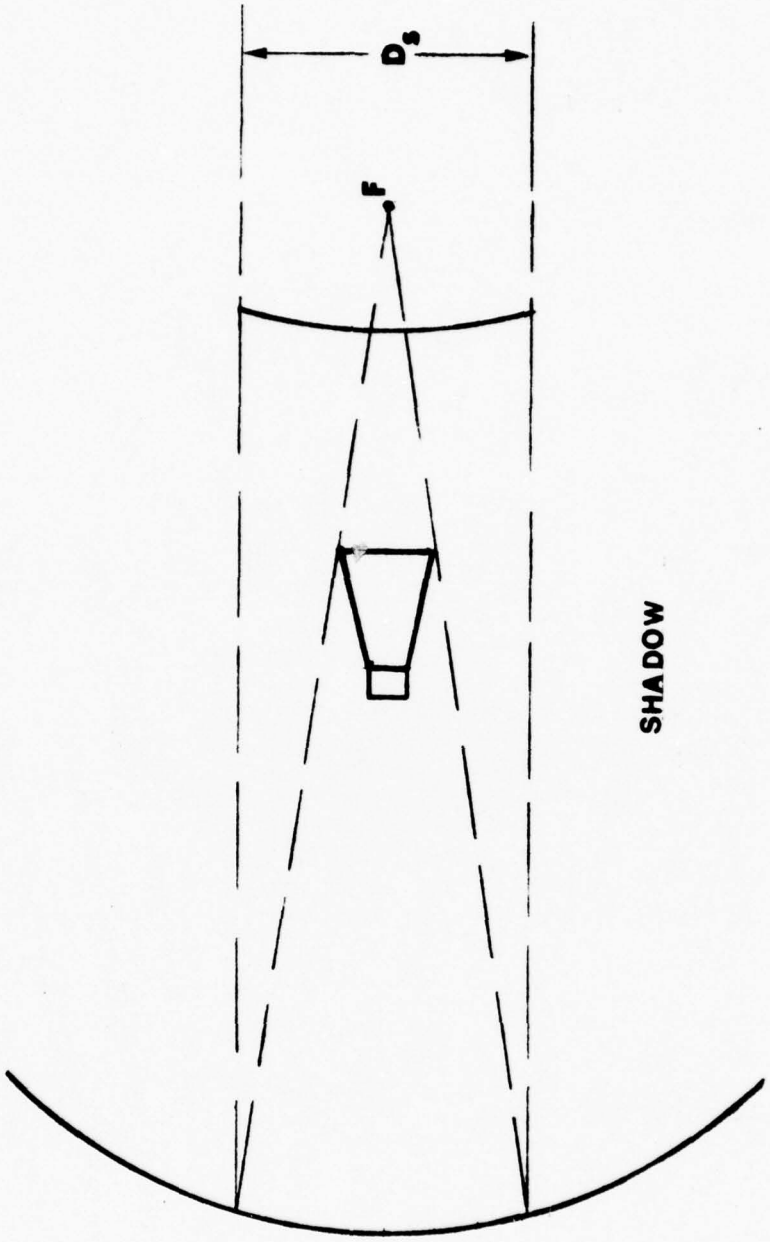

Fig. 2.1. Minimum Blockage Condition.

yields the following expression as an approximation of the subdish diameter which yields minimum blockage:

$$D_s = \sqrt{2F_m\lambda} \qquad (2.3)$$

where D_s is the subdish diameter in centimeters, F_m is the main dish focal length in centimeters, and λ is the radiation wavelength in centimeters. If Eq.(2.3) is divided by the main dish diameter (D_m), an expression for the blockage is obtained:

$$B = \left(\frac{D_s}{D_m}\right) = \left(2\,\frac{F_m/D_m}{D_m/\lambda}\right)^{1/2} \qquad (2.4)$$

where the blockage (B) is defined as the ratio of subdish-to-main dish reflector diameters.

Equation (2.4) is written in this manner to illustrate that, under conditions of minimum blockage, the blockage ratio is a rather simple function of the F_m/D_m ratio of the main dish in wavelengths[5]. Henry has plotted this relationship on a graph of Main Reflector Size in Wavelengths (D_m/λ) versus the Blockage Ratio (B), for F_m/D_m over the range 0.25 through 0.50 (Fig. 3, Page 47 of his paper). This graph is very useful in designing a Cassegrain artenna since it allows an instant approximation of the effects of various changes in frequency on the blockage, and illustrates clearly the assertion

that as the D_m/λ ratio becomes very large, blockage becomes less important[3].

The effect of blockage on antenna gain reduction is given by:

$$G_B = 20\left[\log_{10}(1-2B^2)\right] \tag{2.5}$$

where G_B is the reduction in gain in decibels (db). This relationship permits evaluation of the effects of changes in the blockage ratio, and hence aids in the selection of a design when conflicting criteria must be considered. Table 2.1 shows the results of system calculations based on various blockage ratios, using Eqs.(2.1) through (2.5).

Parameter	Blockage (B)				
	0.100	0.125	0.1354	0.1423	0.2332
F_m/D_m	0.3704	0.3704	0.3704	0.3704	0.3704
D_s (cm)	12.19	15.15	16.51	17.34	28.43
f_d (GHz)	49.15	11.79	9.93	9.0	3.35
G_B (db)	-0.18	-0.28	-0.32	-0.36	-1.0
D_m/λ_d	200	48	40.4	36.6	5.3

Table 2.1. The Dependence of Cassegrain System Parameters as a Function of Blockage

Since the microwave generating equipment available operates in the 8.2 GHz to 12.4 GHz frequency range, the data in the first and last columns of Table 2.1 are of importance only to illustrate the extremes. That is, the values in the first column show that, with a high value for D_m/λ_d, blockage losses are very small, while the figures in the last column indicate that blockage losses become very significant for small values of D_m/λ_d.

The values in the second column were computed using a wavelength of 2.54 cm to find the blockage ratio, because it was known that the radiation wavelength is approximately one inch. The values in the third column were found using the diameter of the available subdish, while the values in the fourth column were found using a design frequency of 9.0 GHz for comparison purposes. The term "design frequency" is of significance only as an approximation, and is not meant to imply an exact operating frequency. By a comparison of the data in the second, third, and fourth columns of Table 2.1, it can be seen that the difference in blockage losses are relatively small, so that any of the subdish diameters could be used satisfactorily. It appeared that a choice of the smaller subdish would yield optimum performance. Since the configuration of the main dish and feed system, as well as

the purpose of the experimental study, dictated that the feed horn be placed between the main dish and the subdish, it was necessary to investigate the possibility of feed horn blockage. This was particularly important since the distance between the feed horn and the subdish would be varied, and changing blockage conditions could negate the value of the experimental results. A geometric model of the system was drawn to scale, and two scale model feed horn profiles were cut out. The shadow of the 15.15 cm diameter subdish and a ray trace from the focal point were drawn as in Fig. 2.1. The feed horn models were placed in the extreme positions that they would occupy during the experiment, and it was determined that vertical blockage would not be affected by the feed horn, but that horizontal blockage would be affected. The same procedure was followed for the 16.51 cm subdish, and the blockage was not affected by the feed horn at all. It was then decided to use that subdish size,

$$D_s = 16.51 \text{ cm}, \tag{2.6}$$

thereby providing another system design parameter.

D. Subdish Design

Since it had been determined that the 16.51 cm subdish would satisfy the minimum blockage conditions, and a subdish of this diameter was available, only the contour of the subdish remained to be verified as that of a hyperbola of prescribed eccentricity. The horizontal depth of the subdish contour (x_s) was measured at three suitable points, y_s = 0, 2.0" and 3.25". Equations (1.2), (1.5), (1.6), (1.7) and (1.8) were then applied with the distance between the foci (F_c) taken to be 12.58" (31.95 cm). This distance is the difference between the focal length of the main dish (F_m), and the approximate phase center of the feed horn. The results showed that the available subdish would not be suitable for use, and had to be redesigned.

Computations were then made using the aforementioned equations varying y_s at one-quarter inch intervals, and the following parameters were obtained:

$$e = 1.53, \qquad \alpha = 16.10^{o}, \text{ and} \qquad L_v = 2.19". \tag{2.7}$$

A new subdish was then fabricated employing the foregoing specifications.

The distance from the focus (F') to the face of the subdish (L_r) was then found by subtracting the value of L_v from the value of F_c. This distance was found to be 10.39" (26.39 cm). The system parameters are summarized in Table 2.2, and illustrated in Fig. 2.2.

Parameter	Symbol	Value
Main Dish Diameter	D_m	121.92 cm
Subdish Diameter	D_s	16.51 cm
Main Dish Half Angle	θ	68.04^o
Subdish Half Angle	α	16.10^o
Main Dish Focal Length	F_m	45.16 cm
Subdish Foci Separation	F_c	31.95 cm
Subdish to Virtual Feed	L_v	5.56 cm

Table 2.2. System Parameters

E. System Assembly

The available struts were suitable for use for mounting the subdish, but were longer than necessary. Shortening the structure forward of the main dish adds mechanical strength, assists in maintaining axial symmetry, and is in keeping with good Cassegrain antenna design procedures. Accordingly, the

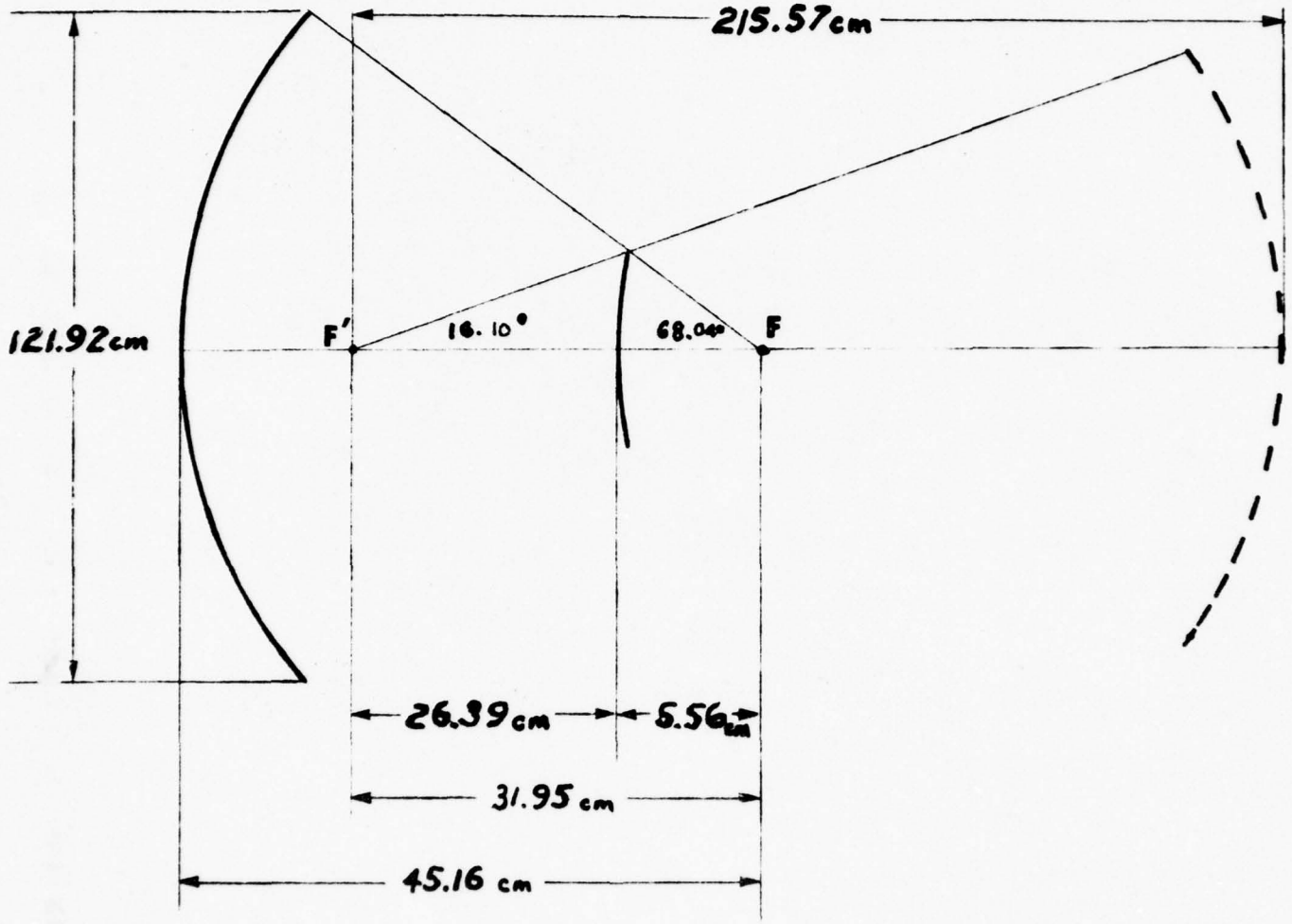

Fig. 2.2. Cassegrain Geometry Details.

struts were shortened, and the subdish was securely mounted and fixed in position.

The feed horn was attached to a length of waveguide which was fed through the center of the main dish, allowing the position of the feed horn relative to the subdish to be varied. A shim was fabricated to be inserted each time the feed horn was repositioned to insure against slippage.

CHAPTER III. EXPERIMENTAL RESULTS

A. Observations

It will be shown, through experimental results reported in this chapter, that spatial oscillations of the "on-axis" rf field with changes in the feed horn-subdish spacing point to the existence of standing waves in the feed horn-subdish region. Several important effects, which might contribute to these observations have also been examined in the present study. Among these are the following:

1. Side lobes in the radiation pattern of Cassegrain antennas are principally associated with forward spillover of the primary feed pattern (i.e., the portion of the primary feed pattern not intercepted by the subdish). The wide-angle radiation produced by these side lobes may, under certain circumstances, create significant oscillations in the amplitude of the received signal when the distance between the transmitting and receiving antennas is changed; a phenomena frequently referred to as "multipath effect."

2. Rearward spillover results from incomplete interception by the parabolic main dish of the energy reflected from the hyperbolic subdish. This energy radiates behind the parabola and is particularly undesirable in low-noise receiving applications (e.g., in deep-space probe tracking and radio astronomy antennas) where the often high ambient noise-level signals reflected from the ground may fall upon the hyperbolic subdish and thereby enter the receiving system; with a consequent degradation of the received-signal signal-to-noise ratio. Furthermore, the configuration of the surfaces behind the Cassegrain antenna can, in certain circumstances, reflect the rearward spillover energy in the forward direction and contribute to multipath effect (because

of interference between the direct and background-reflected signals) when the spacing between the transmitting and receiving antennas is changed. An extreme example of this situation might be that existing when a large, perfectly-conducting reflecting sheet is vertically situated behind either the transmitting or receiving antenna, or both.

3. Calculations show that the hyperbolic subdish lies in the near field of the primary feed horn, and conversely; and, the hyperbolic subdish lies in the near field of the main dish, and conversely. Therefore, as a direct result of this "folded telescope" configuration of the elements making up the Cassegrain antenna, a spatial resonator is formed in the "on-axis" direction of the horn-subdish region; and a second such resonator is formed in the "on-axis" direction of the subdish-main-dish region. A change in the horn-subdish spacing results in significant oscillations in the received signal, as experimental results confirm. Similar oscillations should be expected when the subdish is moved relative to the main dish, but experiments of this type have not been attempted because of the severe defocusing of the entire system which would result whenever the subdish is improperly located.

4. Detailed measurements conducted in the Microwave Laboratory have demonstrated that the vertical and horizontal primary feed horn radiation patterns undergo significant changes when: (a) the horn is completely removed from the parabolic main reflector; (b) the horn is fully back against the inside surface of the parabolic main reflector; (c) the horn is fully forward along the axis of the parabolic main reflector (i.e., farthest from the inside surface of the parabola, along the parabolic axis); and (d) the horn is midway between the extremes of (b) and (c), above. Experimental observations of on-axis oscillations of the radiation pattern, as the horn is slid along the parabolic axis of the main reflector with the subdish removed, cannot be fully taken into account without including the change of the primary feed horn radiation pattern with position along the parabolic axis.

5. On-axis oscillations of the radiation pattern, as the feed horn-subdish distance is changed, may also result, in part, from interaction (i.e., multiple reflections and re-reflections of the radiated signal) between the transmitting and receiving antenna. This effect may become significant when a large aperture receiving antenna is used for measurements made in the Fresnel region of either or both antennas[12].

In addition to these considerations, the Cassegrain system under study is excited by an exponentially-tapered rectangular feed horn which transforms a TE_{10} waveguide mode into a radiation field that illuminates the hyperbolic subdish. Thus, the entire Cassegrain antenna system is initially excited by a vertically-polarized wave (the horn can be rotated 90^{o} to produce horizontally-polarized wave, if desired), which is not only <u>not</u> circularly symmetric but, moreover, the vertical and horizontal planes passing through the center of the parabola do not have the same amplitude distribution (i.e., the same "illumination taper") because the physical aperture in the vertical and horizontal directions are not the same for the feed horn; that is, the height divided by the width is not unity. This condition of "asymmetric illumination" of the hyperbolic subdish and, subsequently, the main parabola itself must be taken into account when properly interpreting the results observed.

In order to assure the highest degree of frequency stability, the klystron was operated in a thermally-isolated waveguide mount with an electronically-regulated power supply. To minimize the possibility of frequency pulling, two load isolators (each of 20 db return loss) were connected in cascade between the klystron signal source and the waveguide feed to the antenna.

B. Equipment and Environment

A block diagram of the equipment used in experimental work is shown in Fig. 3.1, and an equipment list is shown in Table 3.1.

Component	Manufacturer	Model Number	Serial Number
Reflex Klystron	Western Electric	2K25/ 723A/B	#7599438
Power Supply	FIT EE Dept.	N/A	#008076
X-Band Load Isolators	PRD Electronics	1203	#2348 #2349
Wavemeter	F-R Machine Works	X 410A	#147
Standing Wave Indicator	Hewlett-Packard	4158	#007996

Table 3.1. Equipment List

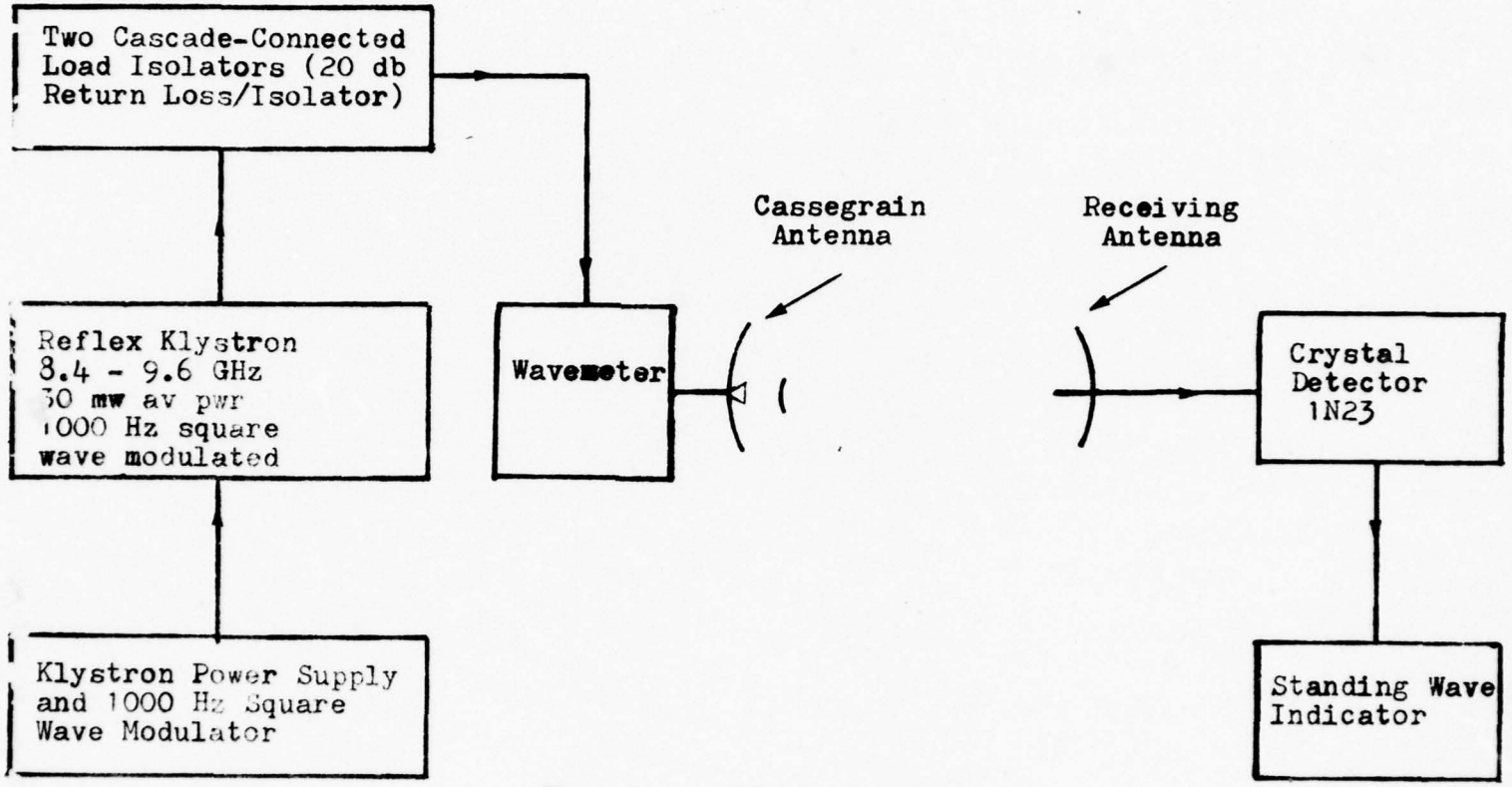

Fig. 3.1. Block Diagram.

The reflex klystron used is tunable between 8.4 GHz and 9.5 GHz, and has an output of 30 mw. The receiving antenna is a dipole driven paraboloid with the same diameter as the Cassegrain.

Measurements were taken in three separate locations, each of which had distinct features. The first series of measurements were taken in an aircraft hangar at Patrick Air Force Base. Although the hangar was quite large, maintenance equipment permanently mounted or stored therein limited the available space. In order to insure against undesirable reflections, it was necessary to restrict the distance between antennas to 75 feet (22.86 meters). A cyclic variation in meter readings was observed during equipment testing. Investigation into the cause of the variations determined that the source of interference was the Airport Surveillance Radar, and that the disturbance was uniform and occurred instantaneously each time the Ground Control Approach radar antenna was directed toward the hangar. Since the magnitude of the disturbance was constant and cyclical, this interference proved to be only a minor annoyance, but did not affect the data taken in this location. The frequency of operation, 9.197 GHz (3.27 cm), assigned by the Frequency Control Officer at Patrick AFB, was chosen to preclude any possibility of inter-

ference with the GCA radar used for landing aircraft.

Subsequent measurements were taken in the F.I.T. Gymnasium and the Microwave Laboratory. The Gymnasium offered several advantages. While it was necessary to remove the equipment on a daily basis, the logistical considerations of such movement was minor compared to the difficulties in moving two large antennas and the associated equipment to and from Patrick AFB. Although the actual playing floor of the Basketball court had to be avoided, the opportunity to move the antennas about, and to achieve a 36% greater separation (i.e., 101 feet, 8 inches) were prime considerations in using that location for those measurements which could not be conducted in the laboratory. The antennas were also raised to reduce the possibility of multipath.

Close range measurements were made in the microwave laboratory. This location was ideal for measurement of close in effects, feed horn radiation patterns, and a design validation approximation using a Helium-Neon Laser as an excitation source.

C. Experimental Technique

The equipment was assembled and allowed to operate for a sufficient length of time to insure stability; i.e., to assure that the system would not undergo significant frequency drifts. Coarse measurements were then taken, and the equipment moved until the possibility of undesirable reflections was eliminated. The antennas were separated from reflecting surfaces, such as walls and equipment not associated with the experiment, so that rearward spillover would be lost, and not reflected back into the area between the antennas. This effectively eliminated a possible source of error.

Once the equipment was in place, and the operating frequency confirmed, on-axis measurements of relative power were taken at ¼ inch intervals (approximately ¼ wave length in the X-Band), by moving the position of the feed horn between measurements. Movement of the feed horn in this manner has the effect of changing the distance between the feed horn and the subdish in ¼ wavelength increments. At the frequency used (9.197 GHz; 3.27 cm), the actual quarter wavelength in free space is 0.32 inch.

Arter the on-axis data was collected, the feed horn was returned to its original position and the antenna radiation

pattern was measured by measuring relative field strength as the receiving antenna was moved in 6" increments to the right and left of the center line, while maintaining a constant antenna separation of seventy-five feet. The radiation pattern was measured in this manner for each of the eighteen feed horn positions.

In order to determine whether multipath effects, or the reception of one or more reflected signals in addition to the desired wave, contributes to the fluctuations expected, and found during the initial experiment, a second set of data was collected. Kraus[9] recommends testing antennas on towers or at the edges of roofs of adjacent buildings to obtain sufficient height to avoid multipath. This approach was found to be impractical for the present investigation because it would require that measurements be taken outdoors, and movement of the antennas by the wind could cause sufficiently strong variations in measured data to suppress the expected effects. The first series of measurements were made at Patrick AFB with the antenna centers 23.26 wavelengths above the floor. For subsequent measurements, the antennas were placed on stands with their centers approximately 5' 9" wavelengths above the floor.

Geometric approximations were made of the effects of multipath on measured data for each of four "worst case" conditions. Figures 3.2a and b show the multipath possibility for the forward spillover at the edge of the subdish for antenna separation of 75 feet and 101 feet 8 inches, respectively. In each case, the path of the reflected signal misses the receiving antenna by several feet (14.56 feet and 16.3 feet respectively). Although it is fully realized that the wave is not in reality a ray, the distances involved are sufficient to conclude that the signal from this part of the forward spillover is not of significant interest. Calculations were made to compute the minimum and maximum grazing angles (β) required for reflected forward spillover to reach the aperture of the main dish. In all cases, this angle was less than 16.01^{o} which indicates that any portion of the feed signal which could be reflected to the receiving antenna would be intercepted by the main dish. Therefore while forward spillover contributes to the side lobes, it cannot be considered to be significant in the multipath case.

Figures 3.2c and d show the multipath condition as applied to the maximum side lobe. In the case of antenna separation of 101 feet 8 inches (Fig. 3.2d), the side lobe passes under the antenna, missing it by 2 feet. In the case of an-

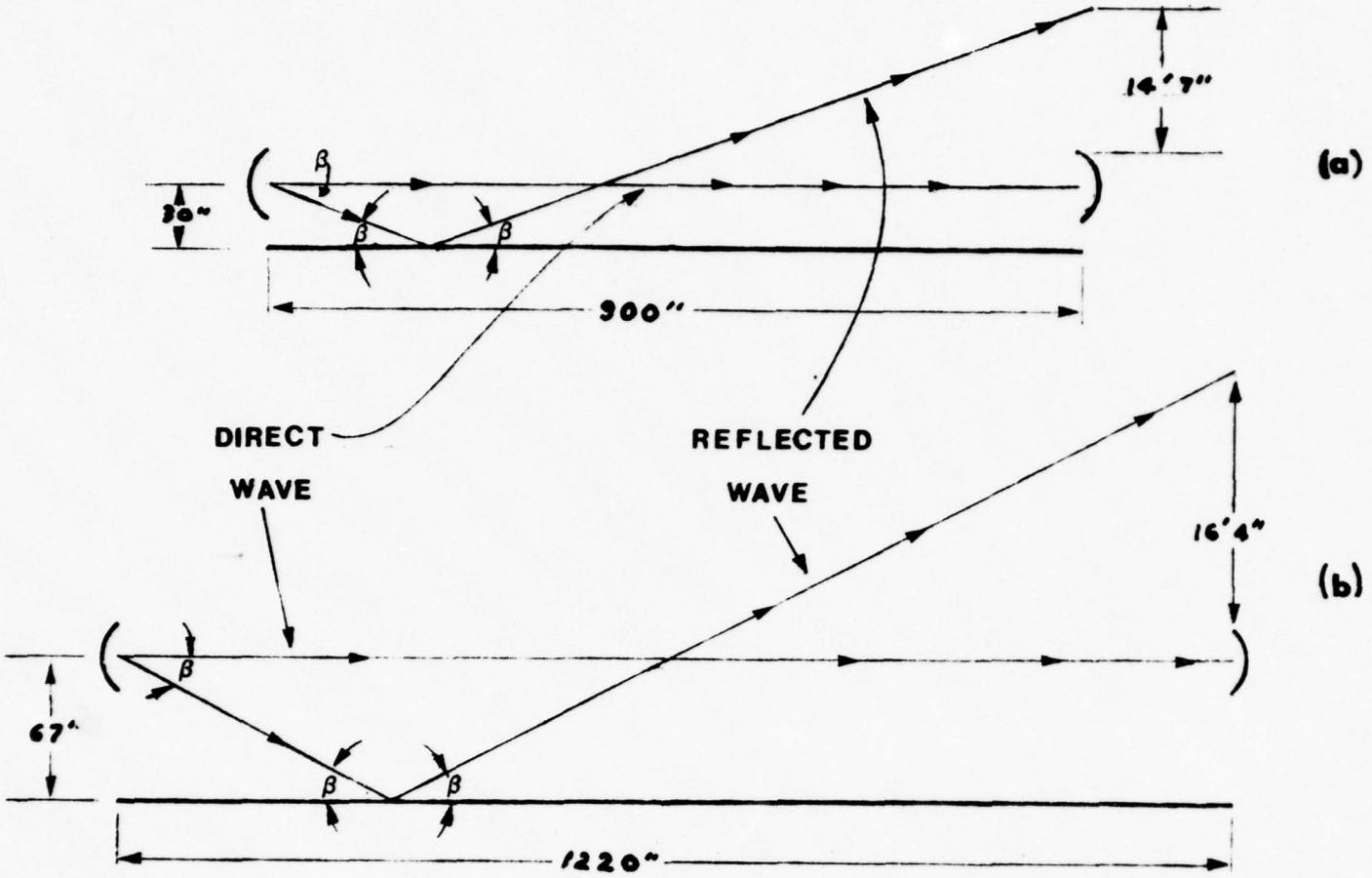

Fig. 3.2. Multipath Geometry - Forward Spillover.
(a) 75 feet. (b) 101 feet, 8 inches.

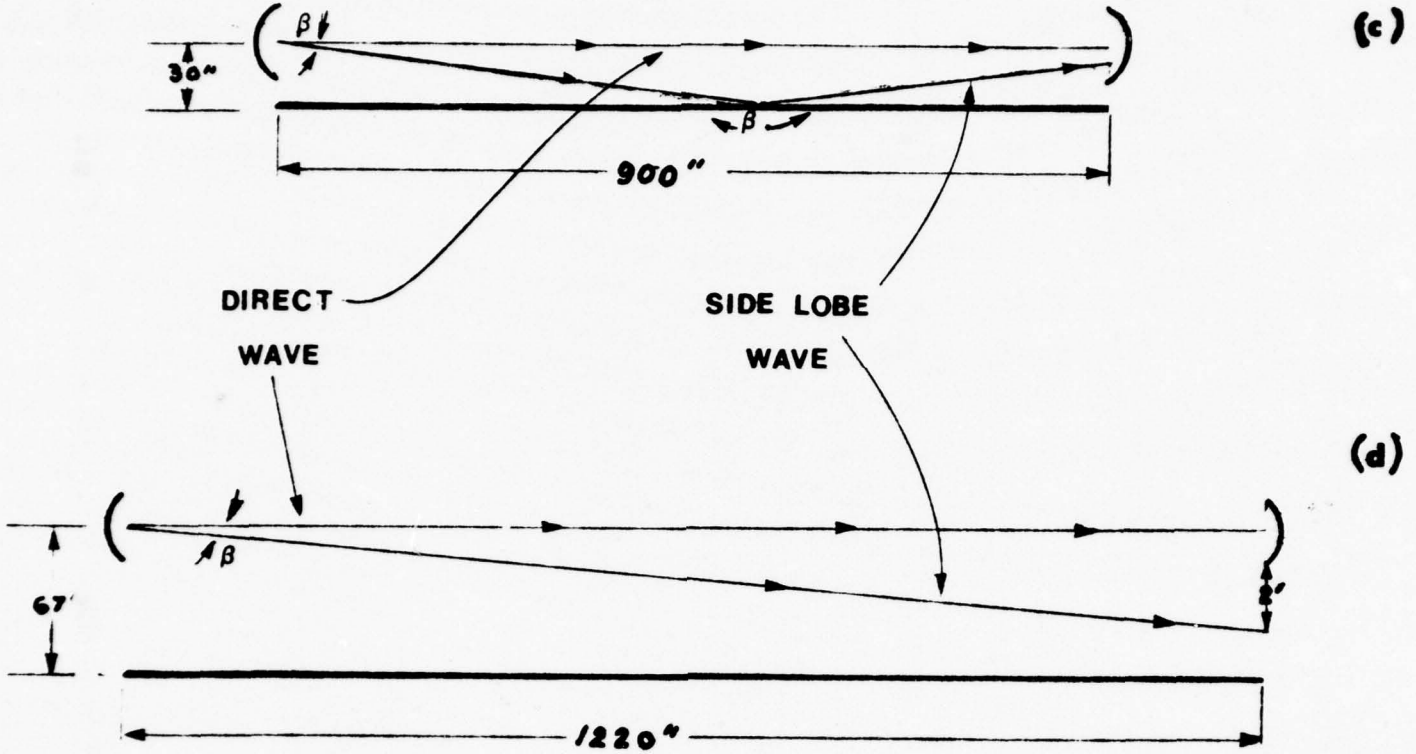

Fig. 3.2. Multipath geometry - side lobe.
(a) 75 feet. (b) 101 feet, 8 inches.

tenna separation of 75 feet, however, the signal could reflect into the receiving antenna. To carry the "worst case" condition forward we will assume that the receiving antenna is 100% efficient, and absorbs all radiation striking the main dish (this, of course, is not the case).

The relative db gain is given by[11]:

$$G = 10 \log_{10} \left(\frac{P_R}{P_D} \right), \tag{3.1}$$

from which,

$$G = 20 \log_{10} \left(\frac{E_R}{E_D} \right) \tag{3.2}$$

can be derived, where P_R is the reflected power, E_R is the reflected electric field, P_D is the direct power, and E_D is the direct electric field at the receiving antenna. The side lobe level is -10.1 db. Substitution into Eq.(3.2) yields:

$$\frac{E_R}{E_D} = 0.3126. \tag{3.3}$$

Since it is known that the electric field intensity varies proportionately to the inverse of the path length between antennas (range), the relative field strengths at the receiving antenna is:

$$E_D = \frac{E_R}{0.3126} \times \frac{r_D}{r_R} \tag{3.4}$$

where r_D and r_R are the lengths of the direct and reflected paths respectively. Over the paths described in Fig. 3.2c,

$$r_D = 900 \text{ inches}; \; r_R = 901.45", \tag{3.5}$$

which results in

$$E_D = \frac{E_R}{0.3131} \tag{3.6}$$

The path lengths given above result in the reflected wave lagging the direct wave by 47.93°. Again assuming the worst case, we will take the signals to be either in phase, or 180° out of phase, we can find by phasor addition that the maximum gain difference between the two cases would be:

$$G = 20 \log_{10} \frac{|E_D| + |E_R|}{|E_D| - |E_R|} \tag{3.7}$$

which yields

$$G = 5.6280 \text{ db}. \tag{3.8}$$

This would be the difference between the maximum and minimum in one cycle in Fig. 3.3. This difference was measured, and found to be 0.6 db. If the phase difference is taken into account and we assume antenna efficiency of 5%, the variation is still on the order of 2.0154 db.

The results of the foregoing calculations are shown in Table 3.2. The argument could be carried further to include tracing of multipath in the case of the main beam, but comparison between the value of one-half the beam width, and the minimum and maximum grazing angles shown in Table 3.2 shows that multipath cannot occur in those cases. Evaluation of the above results shows that multipath effects cannot contribute to the observed oscillations.

Table 3.2. Multipath Factors

	Antenna Separation	
	75 feet	101 ft. 8 in.
Minimum Grazing Angle (β)	3.01°	5.15°
Maximum Grazing Angle (β)	4.66°	7.38°
Distance between antenna and path:		
Forward Spillover	14.56 ft.	16.30 ft.
Side Lobes	N/A	2.01 ft.
Phase Difference in Received Signal	-47.93°	N/A
Magnitude of Oscillations	2.0154 db	N/A

In addition to the measurements described above, the subdish was removed from the Cassegrain antenna, thereby reverting to a standard horn antenna with a background parabolic reflector. Similar measurements were made with this

configuration at two different antenna separation distances.

All subsequent measurements were taken in the Microwave Laboratory. The feed horn was removed from the system, and the radiation pattern was measured at five degree intervals at a distance of 12½ inches. The horn was then replaced in the paraboloid and the radiation pattern was measured with the feed horn in the design position, extended half way, and fully extended. Finally, the subdish was replaced, and on-axis measurements taken at eight feet and eleven feet antenna separation.

D. Experimental Results

The on-axis data taken in the initial experiment was plotted, and an approximating smooth curve was drawn through the data points. The resulting graph of On-Axis Relative Power (db) versus Feed Horn to Subdish Separation (wavelengths) is shown as Fig. 3.3. The expected oscillations are clearly evident, with peaks occurring at, or very near to, half-wavelengths, and negative extremes occurring in the vicinity of half-wavelength plus one-quarter-wavelength points, especially in the mid-range (5.5, 6.0 and 6.5). This behavior clearly indicates the presence of standing waves.

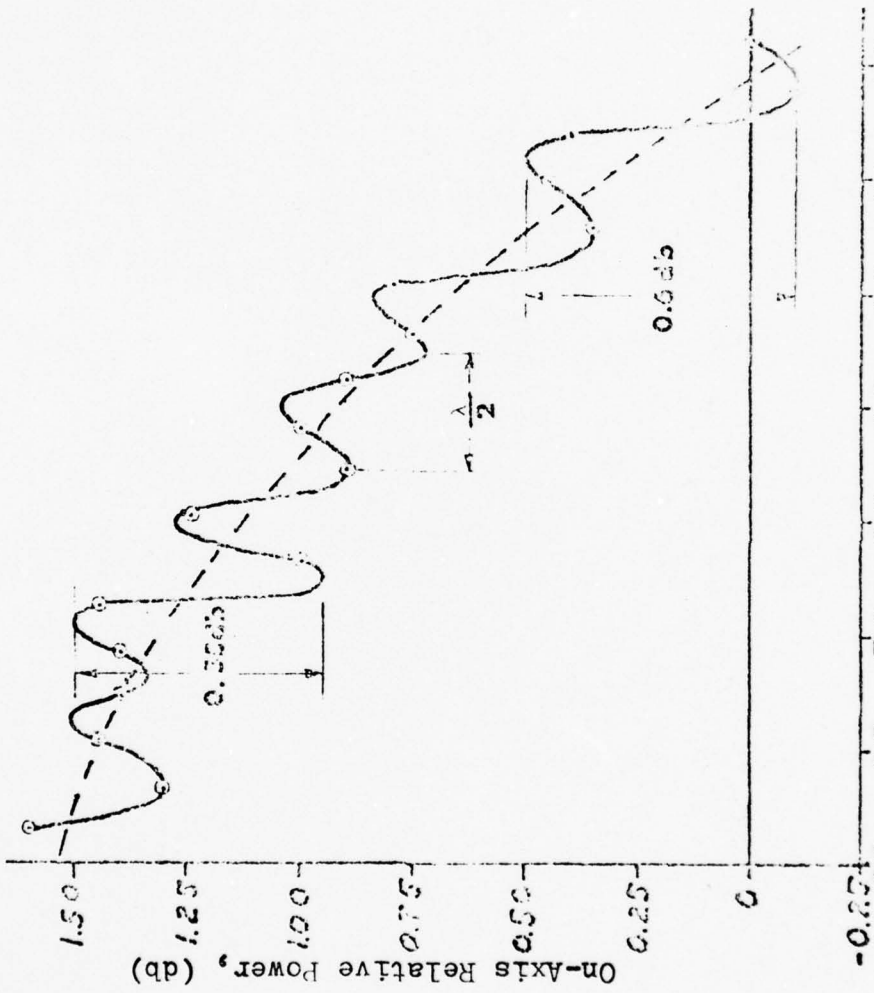

Fig. 3.3. On-Axis Relative Power versus Feed Horn to Subdish separation, 75 feet.

It may at first appear that the oscillations are the result of "defocusing the system" by moving the feed horn, but since the subdish is maintained in a fixed position, the virtual feed is stationary, and the Cassegrain geometry prevails. If the subdish had been moved, the system geometry would have been disturbed, and a degradation of the average signal strength (dotted line in Fig. 3.3) could be expected. It is obvious from examination of Fig. 3.3 that exactly the opposite case applies, resulting in signal strength enhancement as the distance between the feed horn and the subdish is reduced. Careful measurements were made of the relative forward spillover of the subdish, and a plot of data appears as Fig. 3.4. It is apparent that spillover decreases as the feed horn to subdish separation is decreased, resulting in increased power being reflected into the main dish, and hence, the general rise in average power in Fig. 3.3.

The oscillations evident in Fig. 3.3 were originally thought to be solely the result of the effects of a spatial filter similar to a Fabry-Perot resonator existing in the interval between the feed horn and the subdish[2]. Further measurements tend to confirm the existence of such a filter, but also indicated the necessity of considering the effects of the possible contributing factors described in the first section of this chapter.

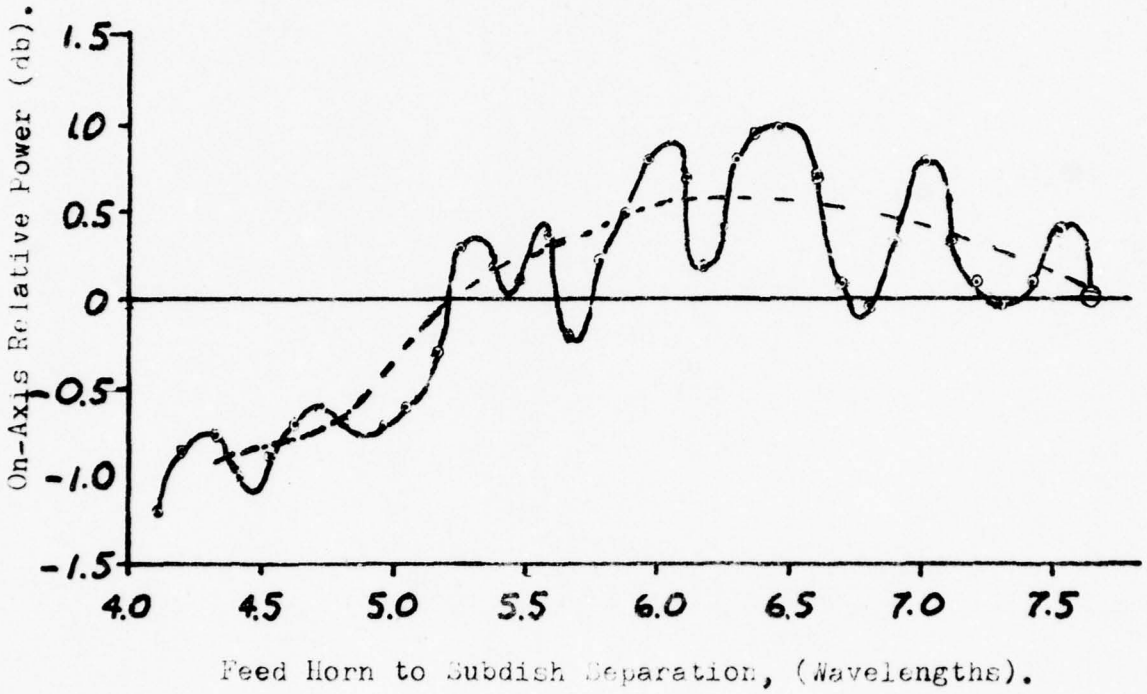

Fig. 3.4. Forward Spillover - Relative Power versus Feed Horn to Subdish Separation.

The on-axis data recorded during the second and third experimental sessions were plotted, and are shown as Figs. 3.5a, b and c. Examination of Fig. 3.5a, and comparison with Fig. 3.3 reveals that the general waveshape is identical, but that a slight shift in phase occurs, reaching one-half-wavelength as the minimum separation is reached. The general reduction in average signal strength can be expected as a result of the 36% increase in antenna separation with no offsetting increase in transmitted power.

The antennas were brought into close proximity in the laboratory, and on-axis data taken and plotted in Fig. 3.5b and c. The variations in relative amplitude and period seen in these two cases are the result of interaction between the two antennas. As the wave arrives at the receiving antenna, part of its power is absorbed by the antenna, and the remainder is scattered. A portion of the scattered power is reflected back toward the transmitting antenna, and when the antennas are sufficiently close, is reflected again, etc.[13] A similar phenomenon is common in optics in the case of interference between two reflectors[14].

In order to avoid antenna interaction, measurements should be taken in the Fraunhofer region, or the far field, if possible. Separation of the antennas will eliminate the

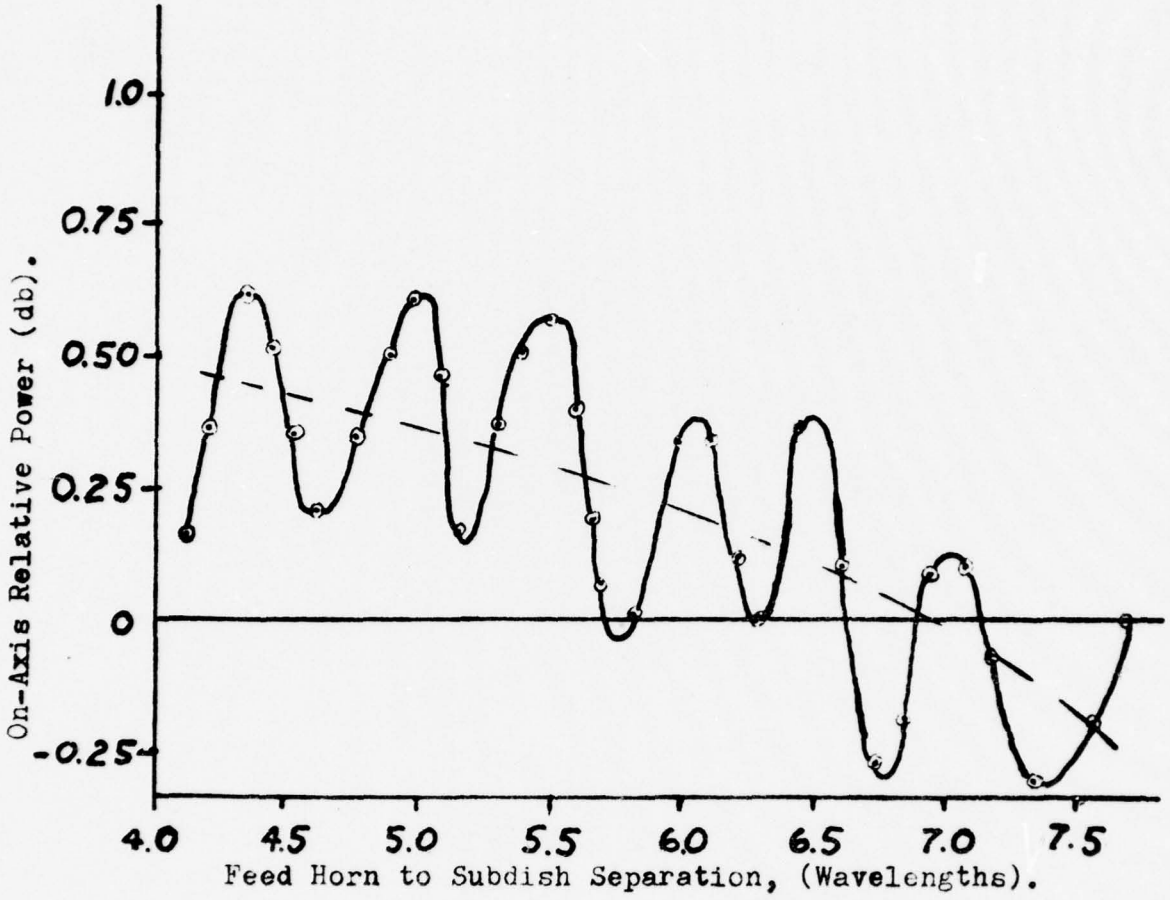

Fig. 3.5a. On-Axis Relative Power versus Feed Horn to Subdish Separation, 101 feet, 8 inches.

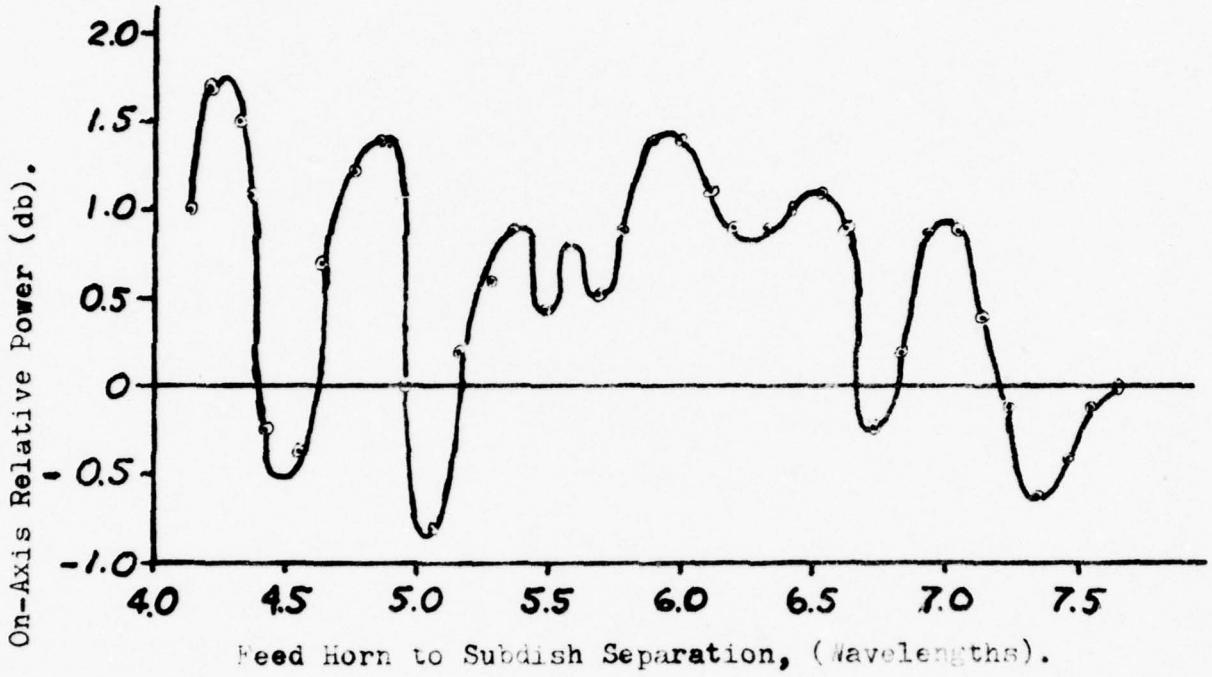

Fig. 3.5b. On-Axis Relative Power versus Feed Horn to Subdish Separation, 11 Feet.

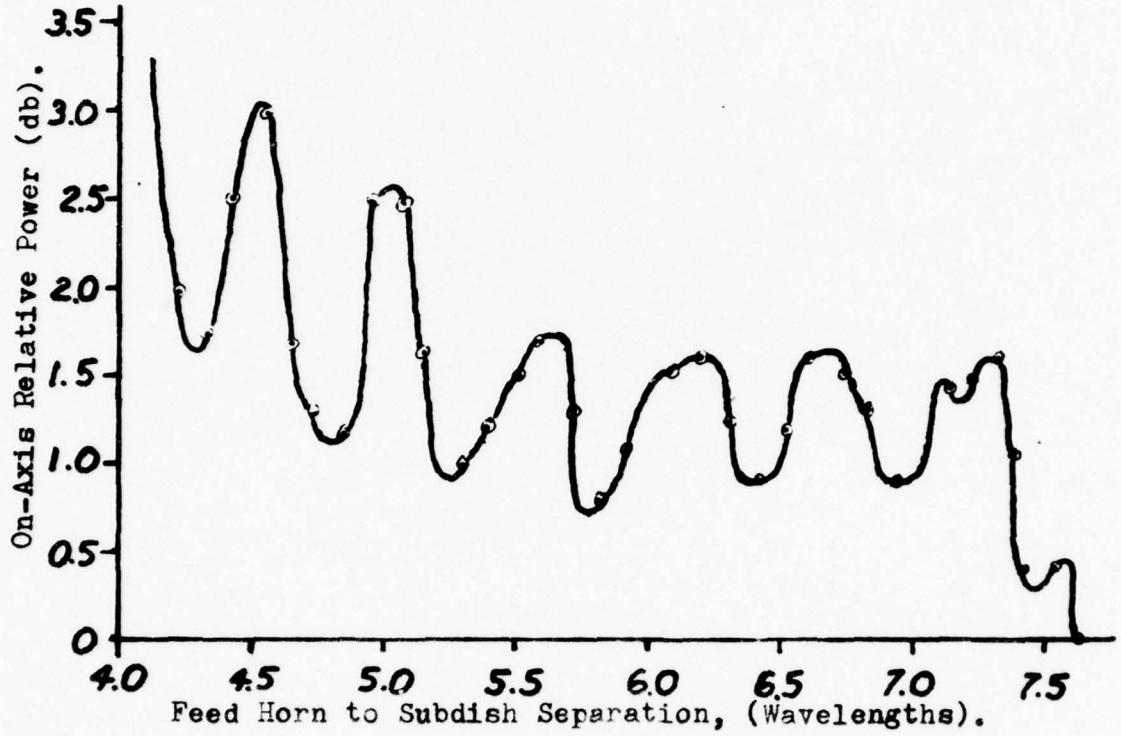

Fig. 3.5c. On-Axis Relative Power versus Feed Horn to Subdish Separation, 8feet.

possibility of interaction between antennas as a possible causative factor. The approximate Fresnel-Fraunhofer Boundary is computed[12] from the relation:

$$R_c = \frac{2D_m^2}{\lambda} \tag{3.9}$$

For the antenna under study, the diameter is 121.92 cm, and the wavelength for 9.197 GHz is 3.27 cm, yielding:

$$R_c \approx 91.23\text{m} \ (300\text{ft}). \tag{3.10}$$

Considering the entire frequency range of the equipment, 8.2 GHz to 12.4 GHz, the Fresnel-Fraunhofer Region may vary from 266.95 to 403.69 feet. The above distances consider the use of approximately equal aperture transmitting and receiving antennas, and may be reduced by using an antenna with a smaller aperture for measurements. In either case, an equipment modification would be required. A power amplifier would be required to increase the signal level sufficiently so that it may be detected at these distances.

The radiation pattern measured in each portion of the experimental work was plotted on polar coordinate graph paper. These plots are shown in Figs. 3.6a through [illegible] are organized as follows:

a. Feed horn pattern, vertical polarization.

b. Feed horn pattern, horizontal polarization.

c. Total feed pattern, vertical polarization, with feed horn in design position.

d. Total feed pattern, horizontal polarization, with feed horn in design position.

e. Cassegrain antenna pattern, vertical polarization, feed horn in design position.

f. Total feed pattern, vertical polarization, with feed horn displaced 2¼ inches forward.

g. Total feed pattern, horizontal polarization, with feed horn displaced 2¼ inches forward.

h. Cassegrain antenna pattern, vertical polarization, feed horn displaced 2¼ inches forward.

i. Total feed pattern, vertical polarization, with feed horn displaced 4¼ inches forward.

j. Total feed pattern, horizontal polarization, with feed horn displaced 4¼ inches forward.

k. Cassegrain antenna pattern, vertical polarization, feed horn displaced 4¼ inches forward.

l. Cassegrain antenna pattern, horizontal polarization, feed horn displaced 4¼ inches forward.

Examination of the radiation patterns in Fig. 3.6a through l illustrates the effect of changes in the feed horn to subdish separation. Figures 3.6c, f and i show the amplification and shaping of the vertically polarized feed horn pattern, while Figs. 3.6d, g and j illustrate the same effect on the horizontal feed horn pattern.

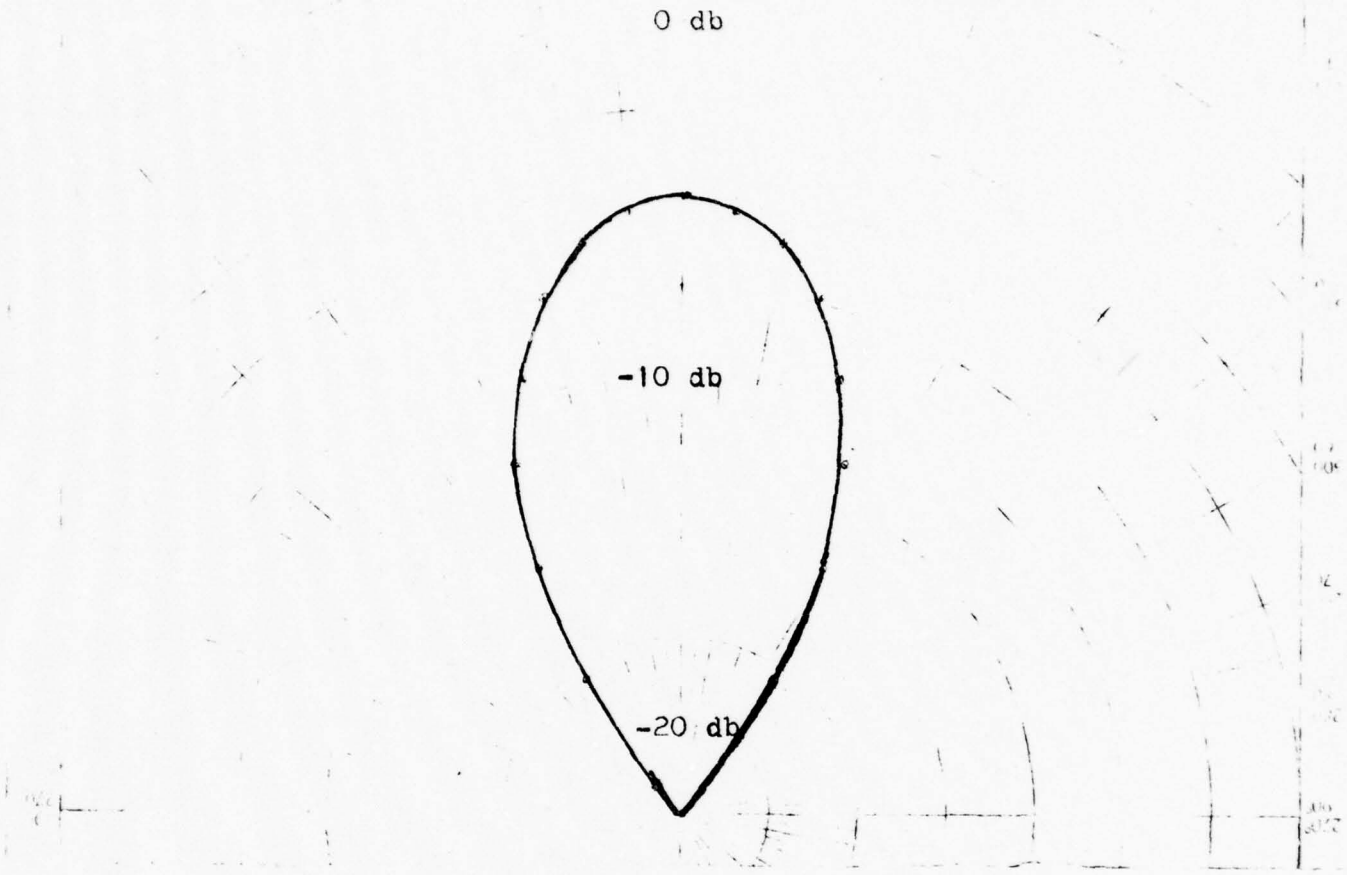

Fig. 3.6a. Feed horn pattern, vertical polarization.

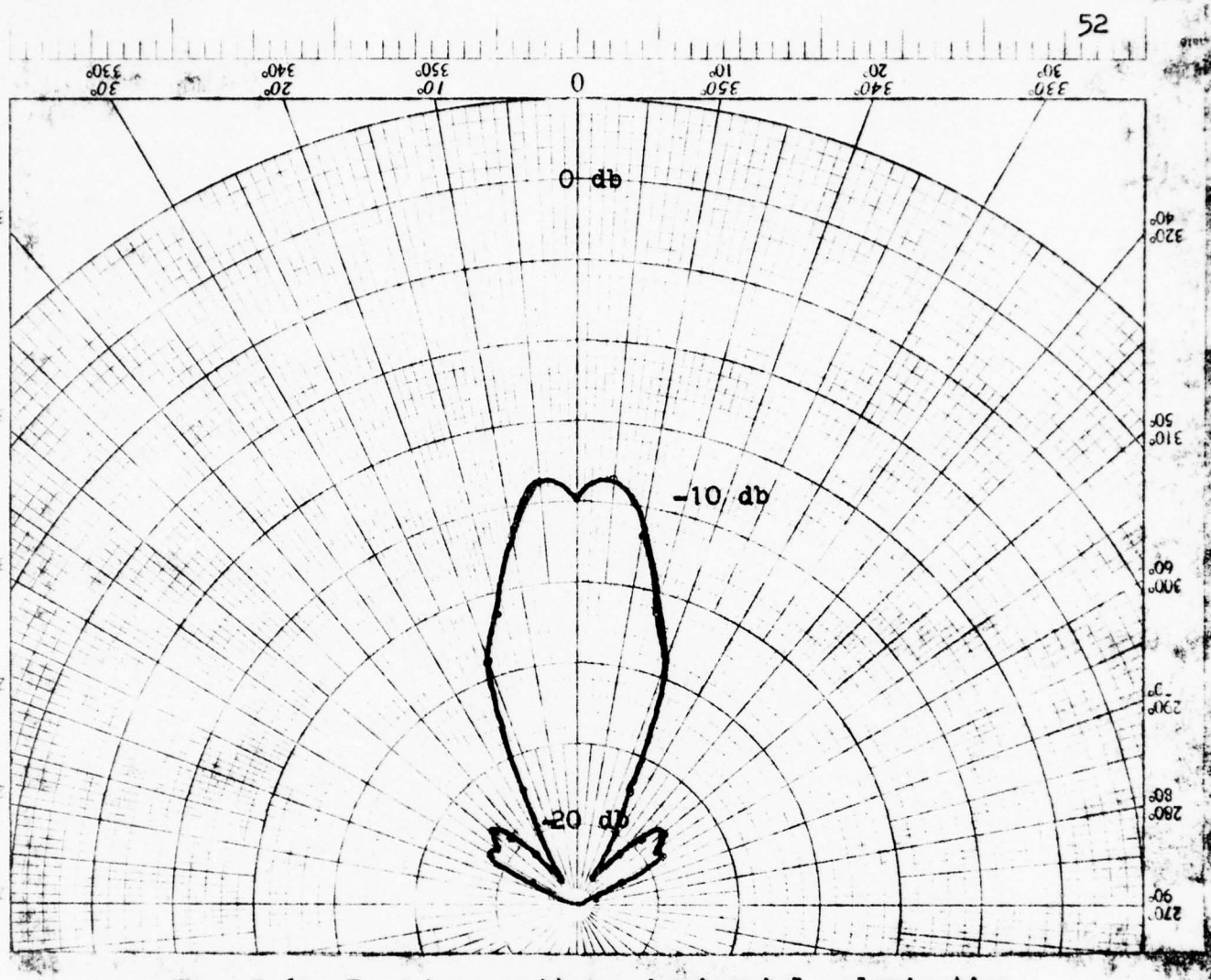

Fig. 3.6b. Feed horn pattern, horizontal polarization.

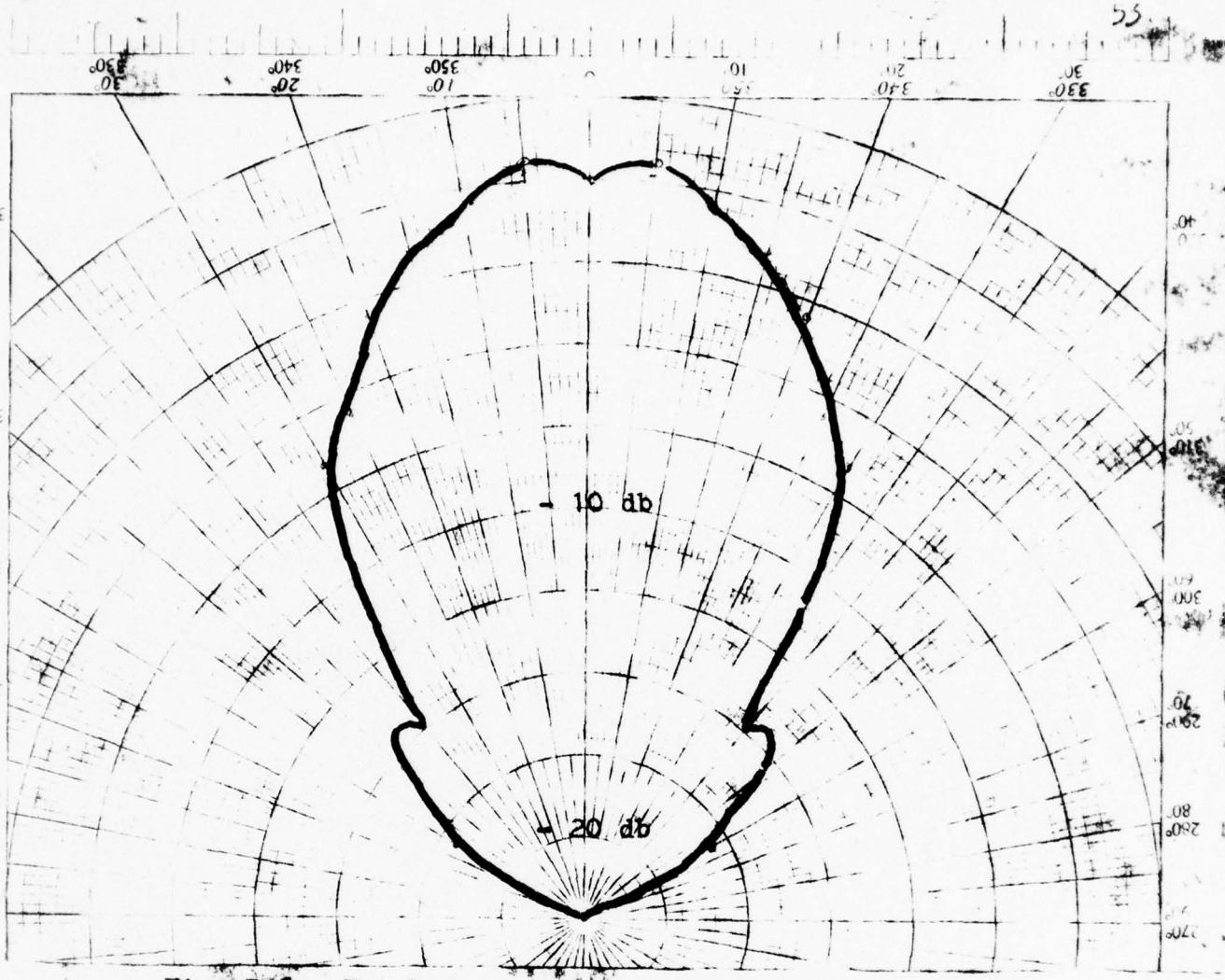

Fig. 36c. Total feed pattern, vertical polarization, with feed horn in design position.

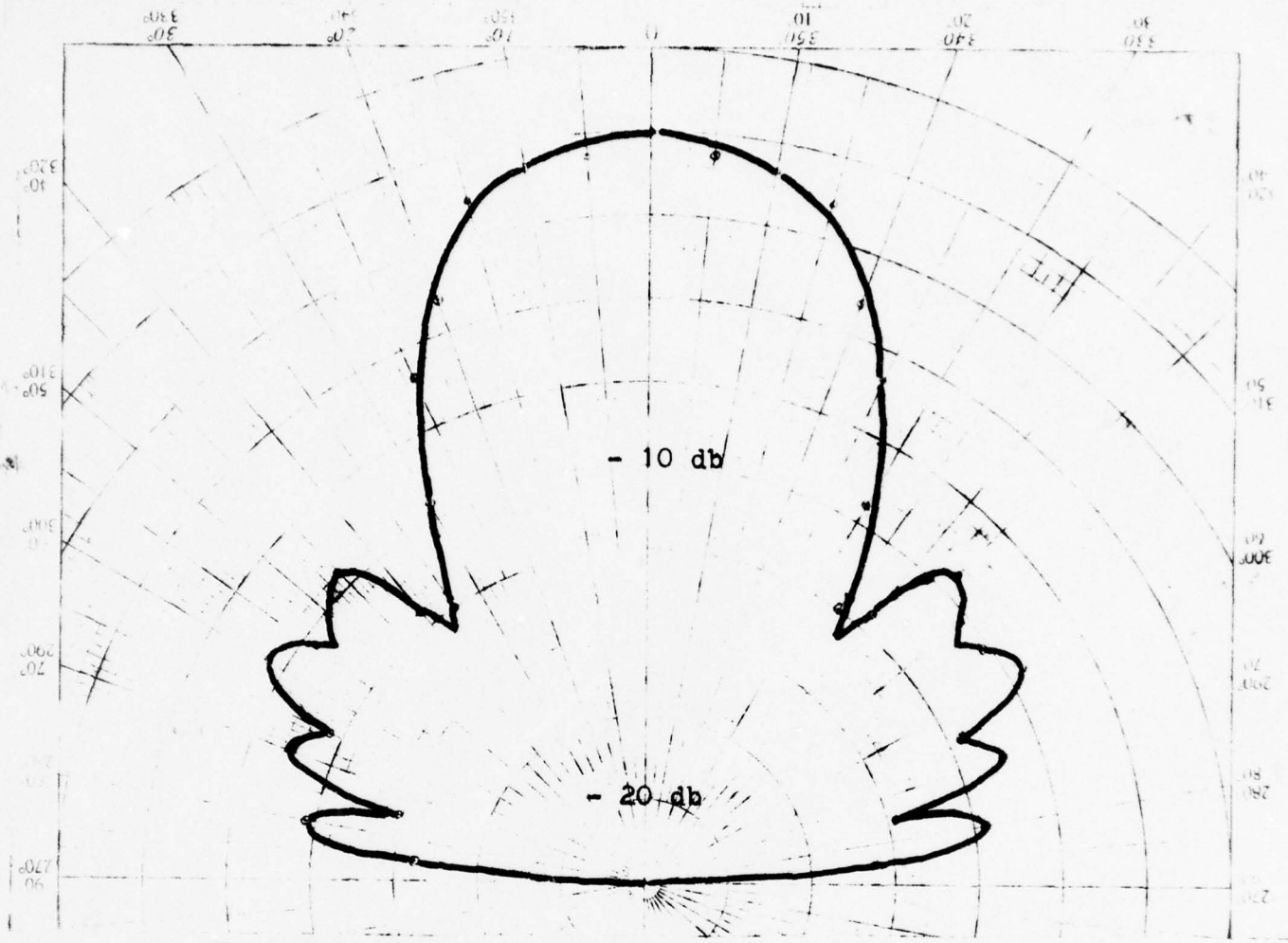

Fig. 3.6d. Total feed pattern, horizontal polarization, with feed horn in design position.

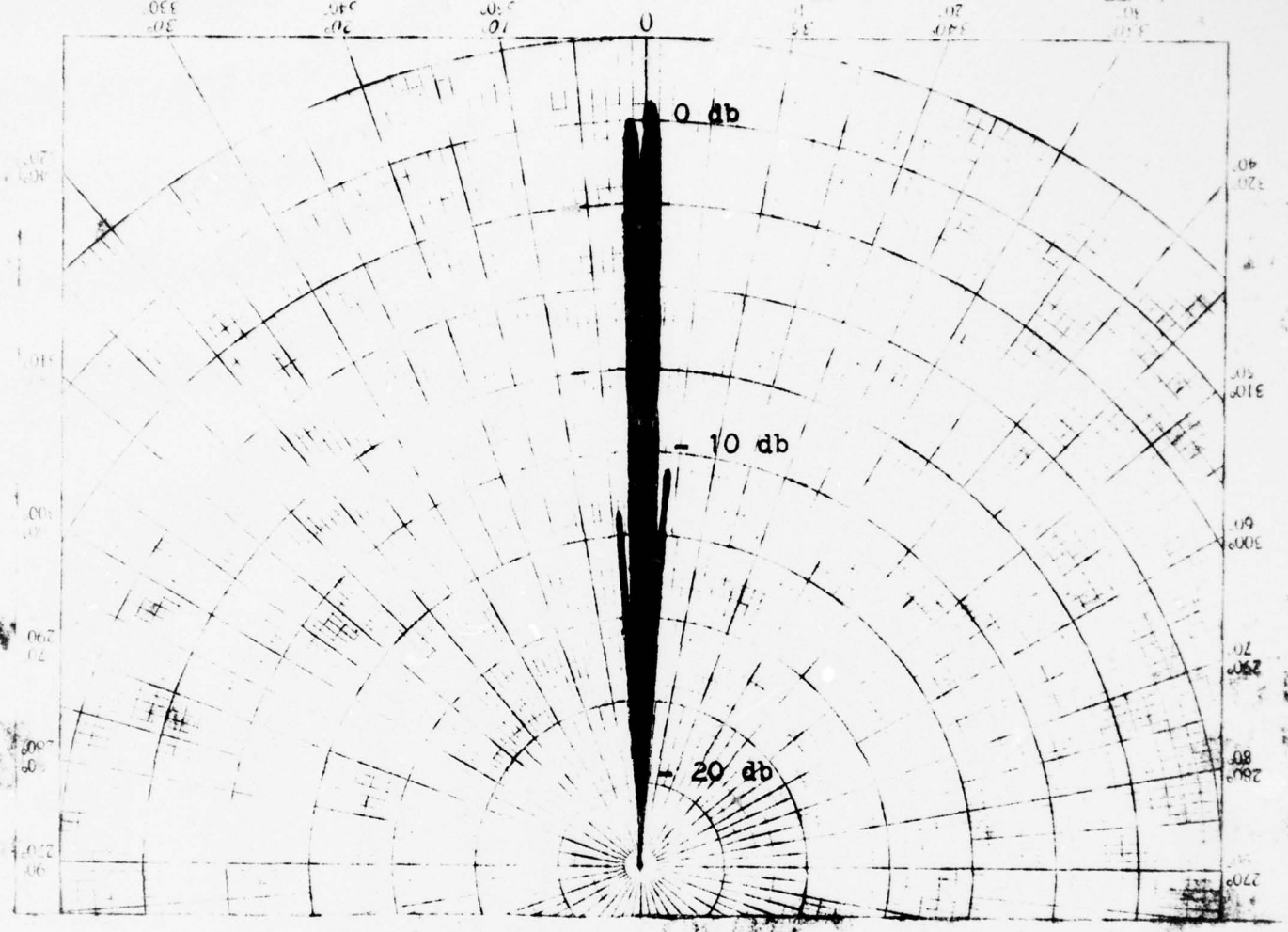

Fig. 3.6e. Cassegrain Antenna radiation pattern, vertical polarization, feed horn in design position.

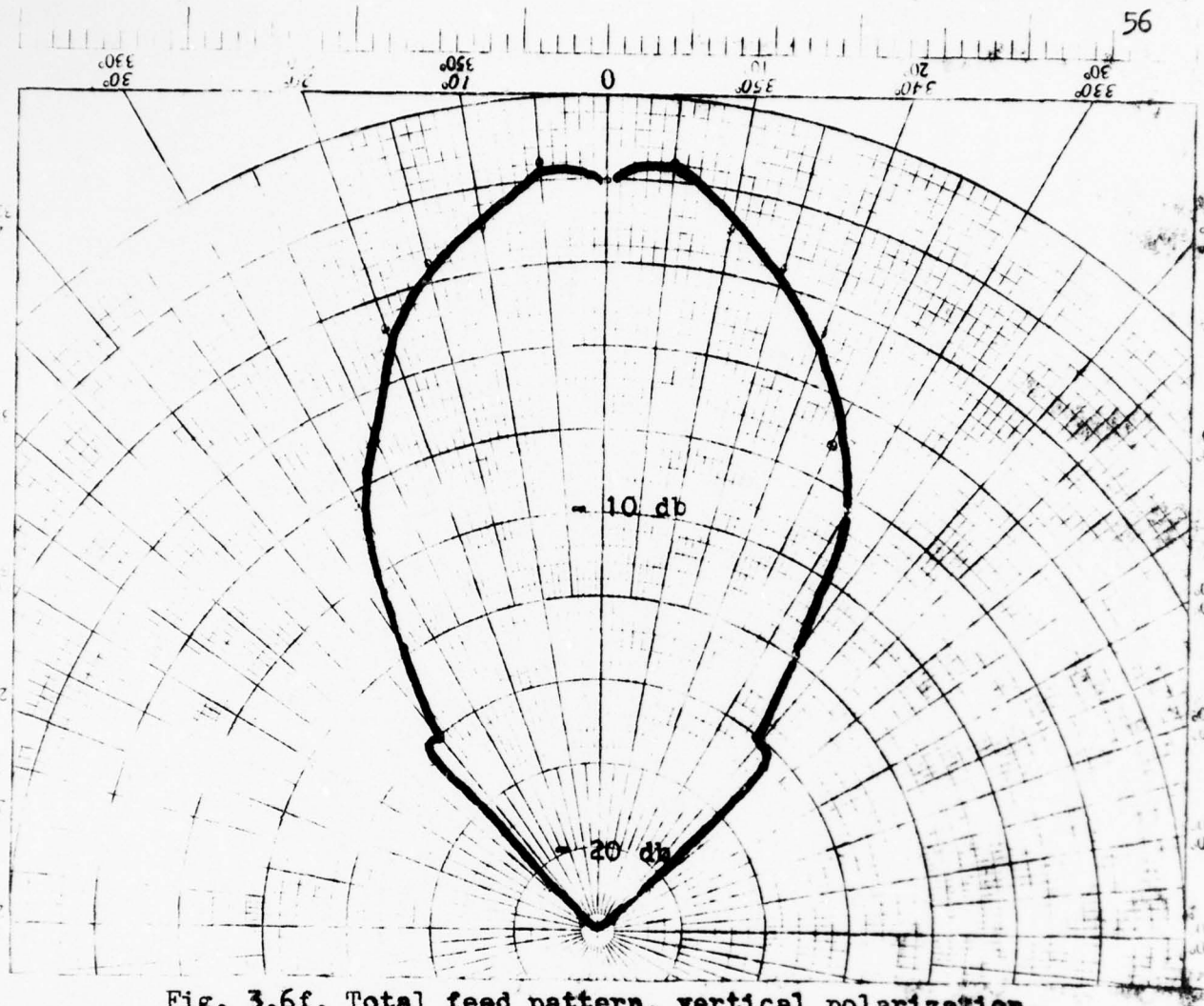

Fig. 3.6f. Total feed pattern, vertical polarization, feed horn displaced 2 1/4 inches forward.

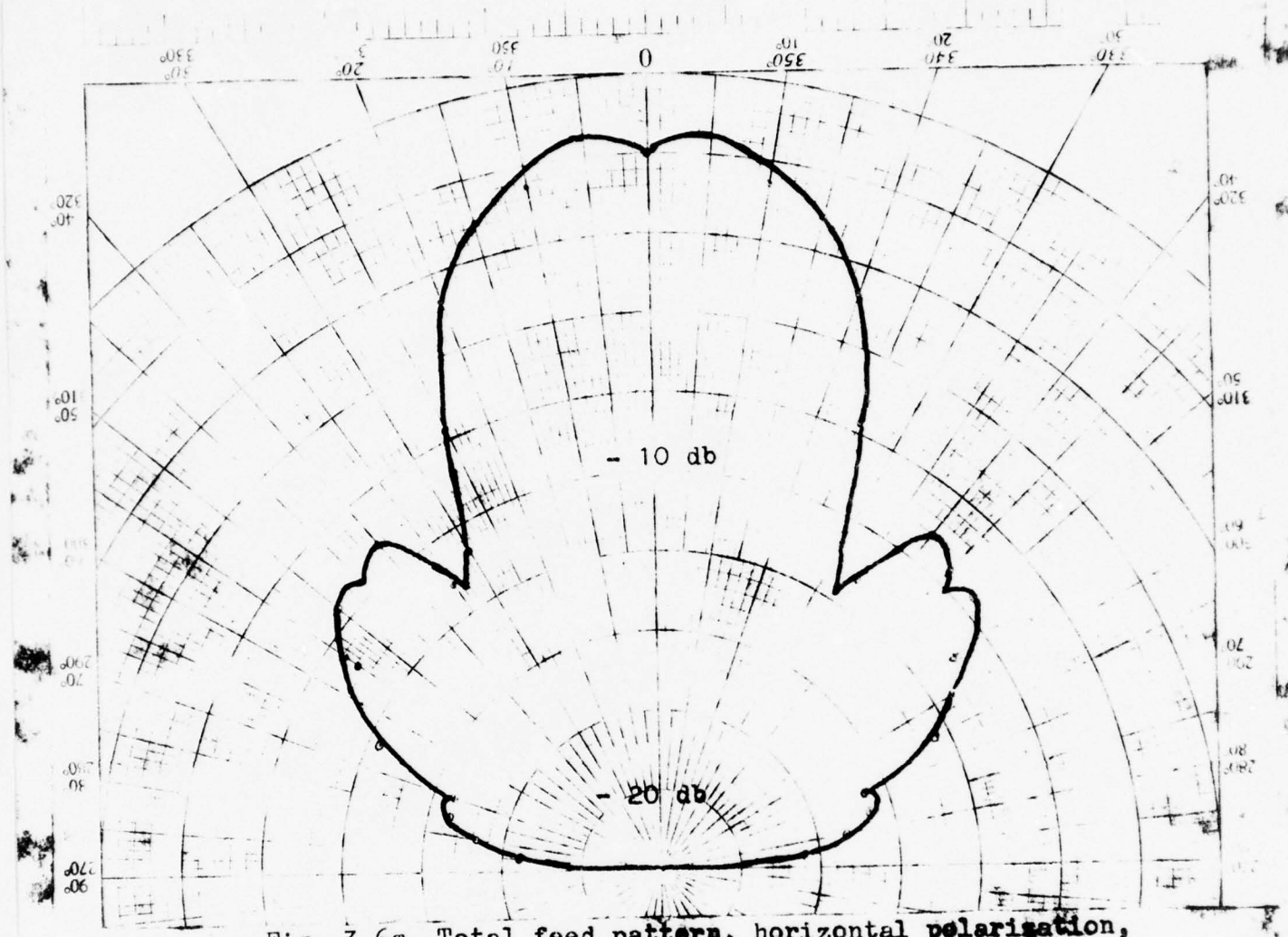

Fig. 3.6g. Total feed pattern, horizontal polarisation, feed horn displaced 2 1/4 inches forward.

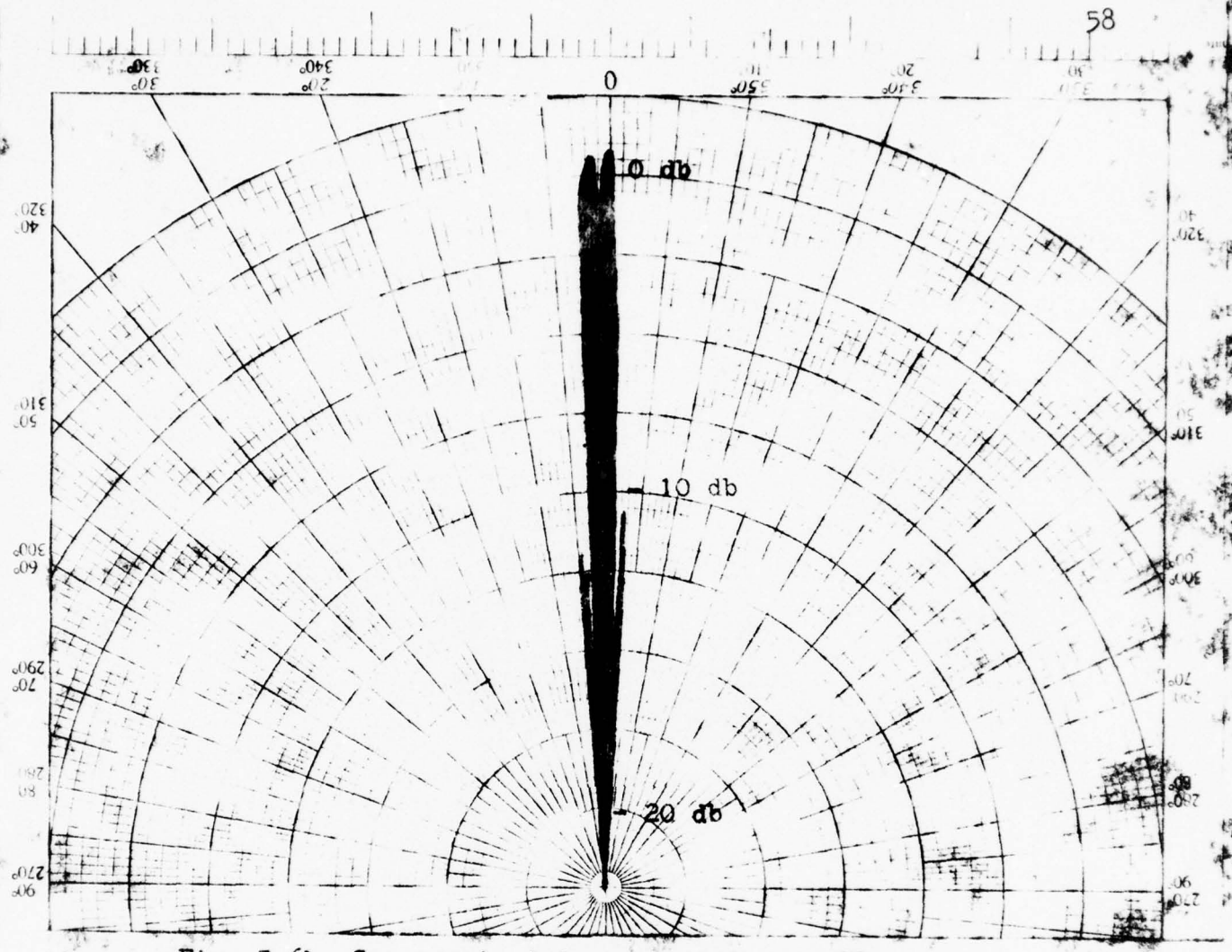

Fig. 3.6h. Cassegrain Antenna radiation pattern, vertical polarization, feed horn displaced 2 1/4 inches.

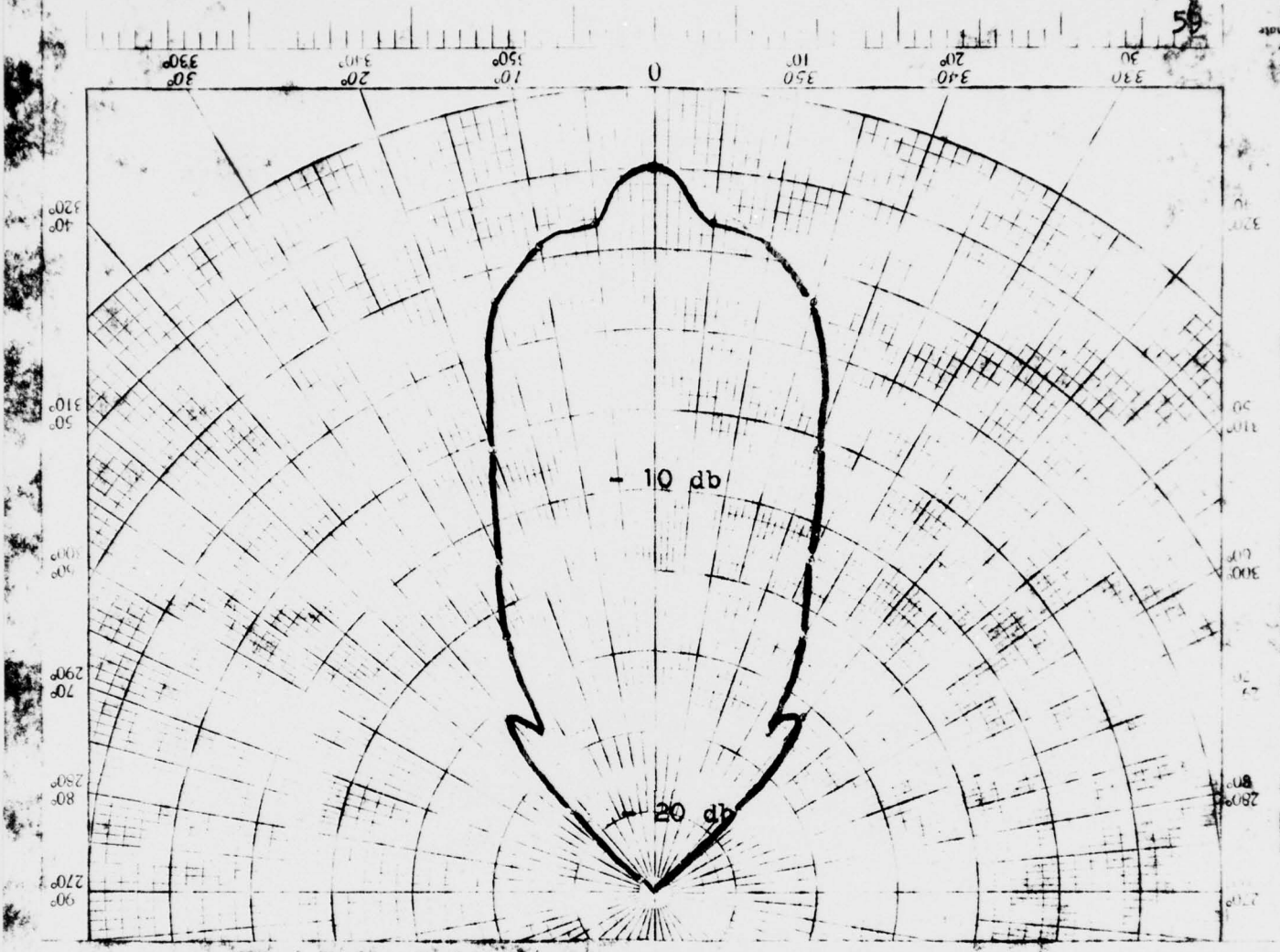

Fig. 3.61. Total feed pattern, vertical polarization, feed horn displaced 4 1/4 inches forward.

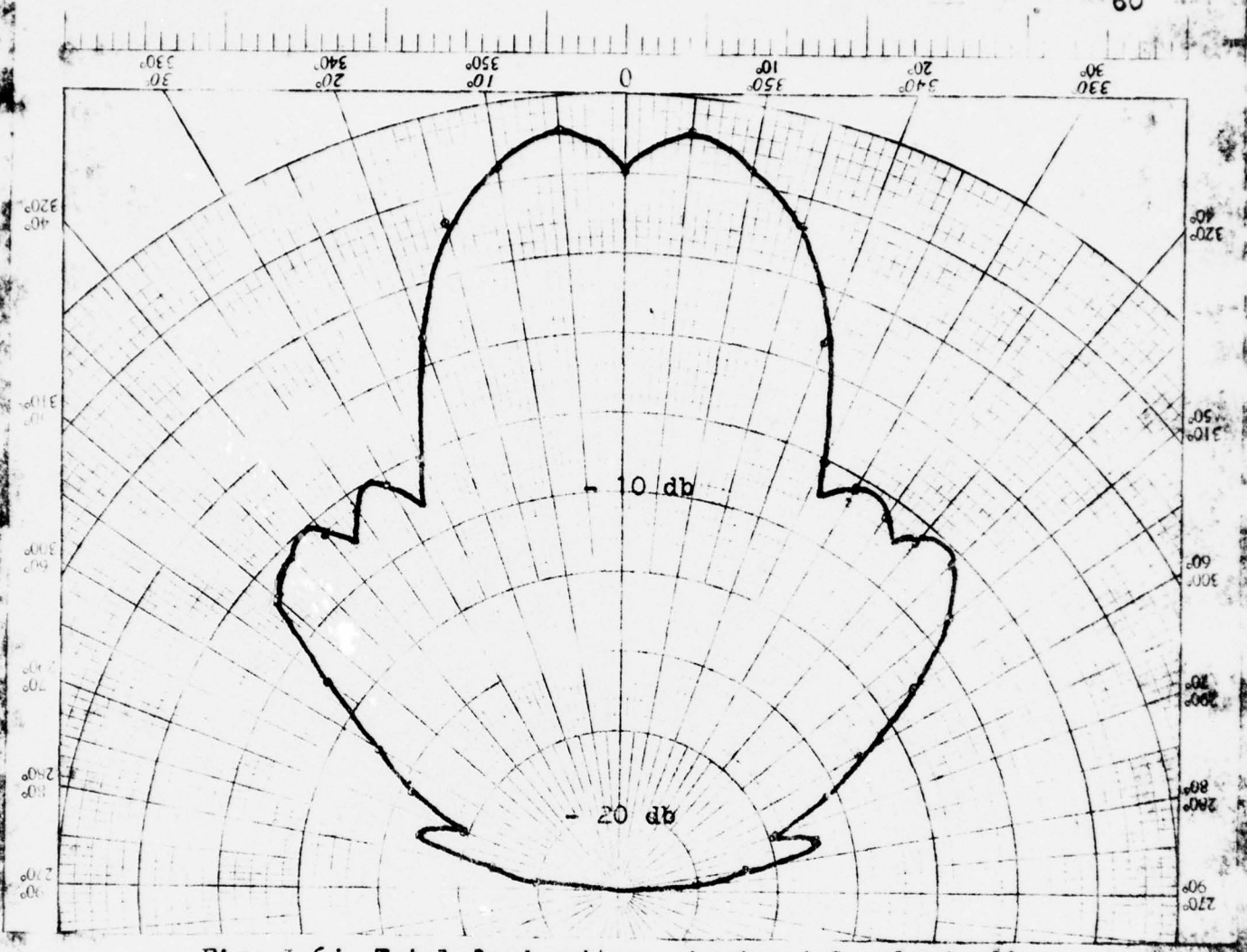

Fig. 3.6j. Total feed pattern, horizontal polarization, feed horn displaced 4 1/4 inches forward.

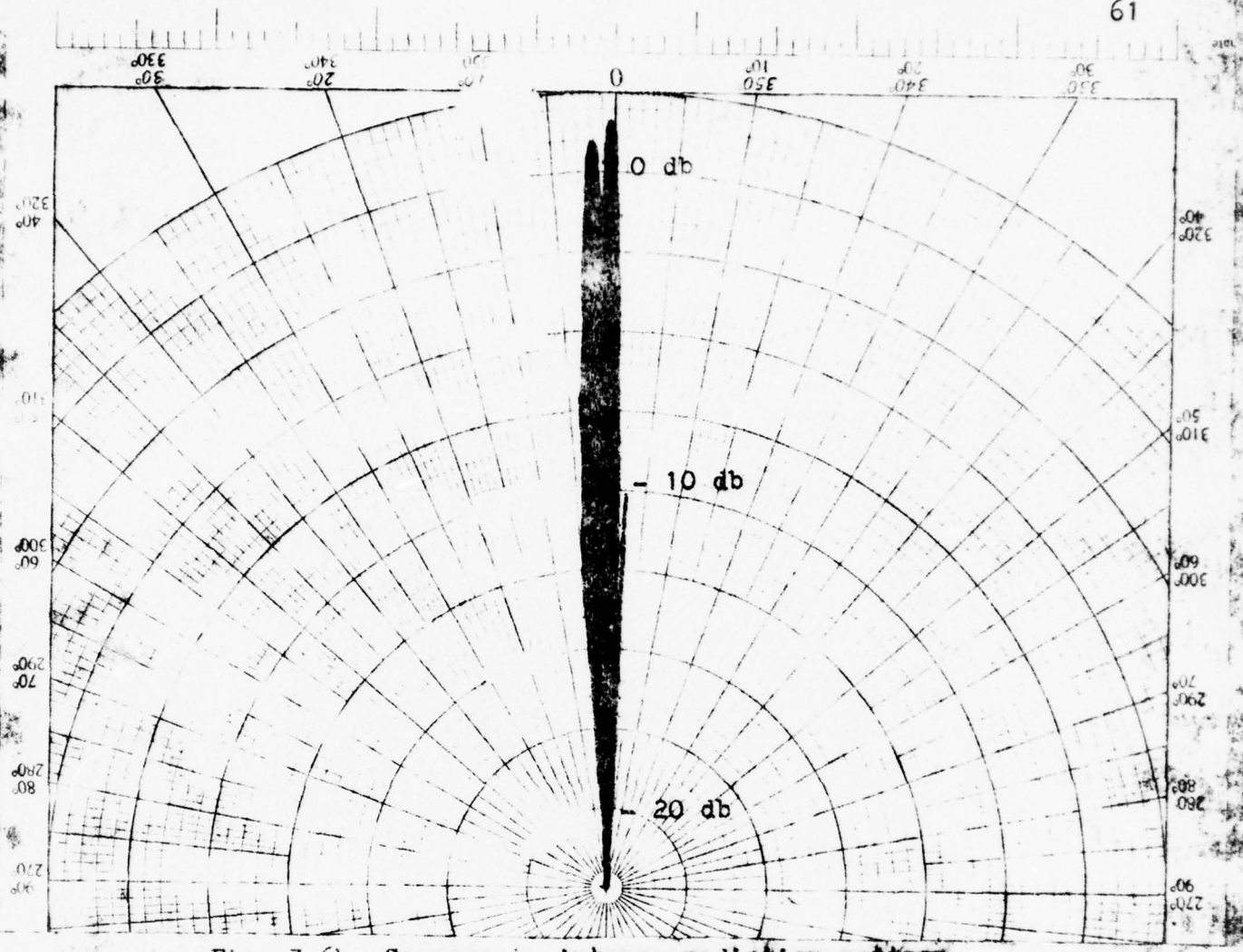

Fig. 3.6k. Cassegrain Antenna radiation pattern, vertical polarization, feed horn displaced 4 1/4 inches.

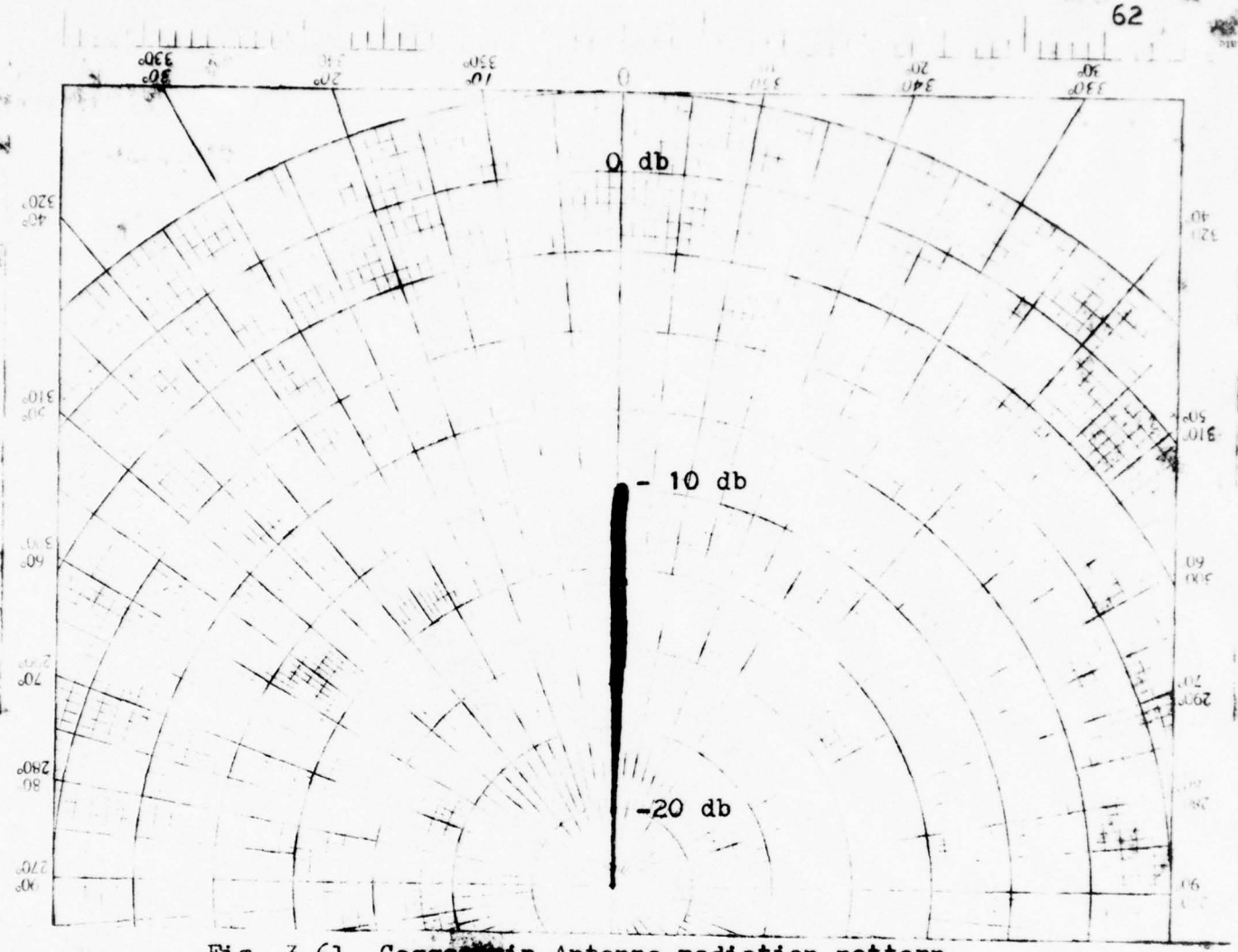

Fig. 3.61. Cassegrain Antenna radiation pattern, horizontal polarization, feed horn displaced 4 1/4 inches.

Figures 3.6e, h and k illustrate changes in the relative power and antenna patterns of the Cassegrain antenna, with the pattern of Fig. 3.6k indicating a 1.0 db increase over the design pattern of Fig. 3.6e. The gain of one antenna over that of a reference antenna is given by[9]:

$$G = 10 \log_{10} \frac{P_2}{P_1} \tag{3.11}$$

where P_2 is the power of the antenna under test, and P_1 is the power of the reference antenna. Substitution yields:

$$\frac{P_2}{P_1} = 1.26 \, . \tag{3.12}$$

The preceding calculation indicates that the antenna gain is increased by 26% by moving the feed horn 4¼ inches forward of its design position, bringing it closer to the subdish. Examination of other radiation plots shows that the relative power varies greatly as the relative position of the feed horn and the subdish is changed. A radiation pattern of the antenna was measured for the design configuration at a second frequency (9.265 GHz). This plot is shown as Fig. 3.7, and shows that there is a considerable increase in relative power at 9.265 GHz as compared to 9.297 GHz (on the order of 2.0 db).

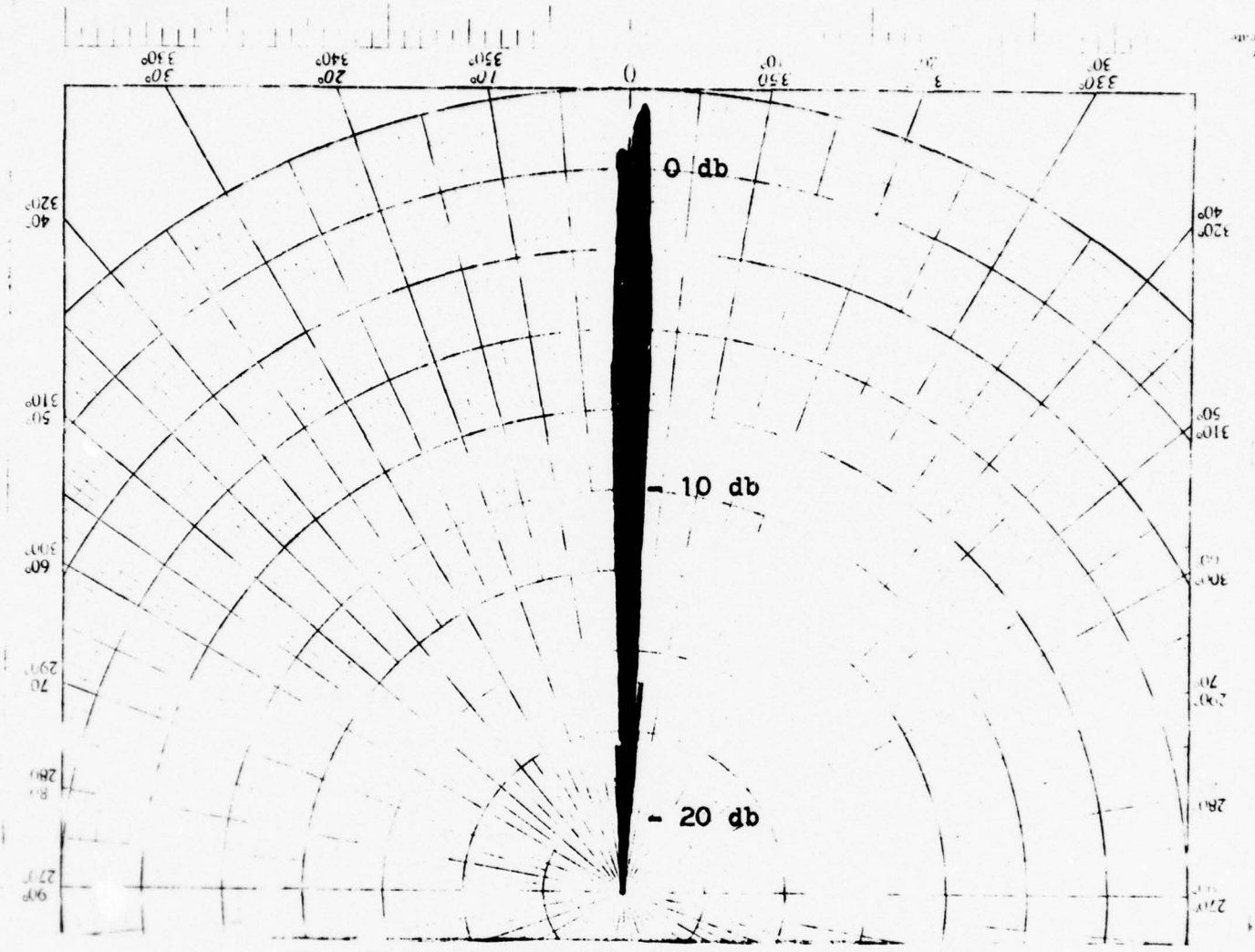

Fig. 3.7. Cassegrain Antenna radiation pattern, vertical polarization-75 feet.

The results of movement of the feed horn relative to tha main dish in the absence of the subdish are shown in Figs. 3.8a and b. Oscillation shifting in phase as the feed horn is moved are clearly evident. These phase shifts are the result of the combination of the direct and reflected waves in the paraboloid.

Antenna performance may be described by a series of inter-related factors: Beam area (B_m), Directivity (D), Effective Aperture in square inches (A_e), and Gain in db (G). The following formulae are used to find the values of these performance factors[11]:

$$B_m = \phi_1 \psi_1 \tag{3.13}$$

where ϕ_1 and ψ_1 are the half power beam widths respectively,

$$D = \frac{41{,}253}{B_m} \tag{3.14}$$

$$A_e = \frac{D\lambda^2}{4\pi} \tag{3.15}$$

and

$$G = 10 \log_{10} G_o. \tag{3.16}$$

G_o is the gain found as a function of directivity, and is found by:

$$G_o = kD \tag{3.17}$$

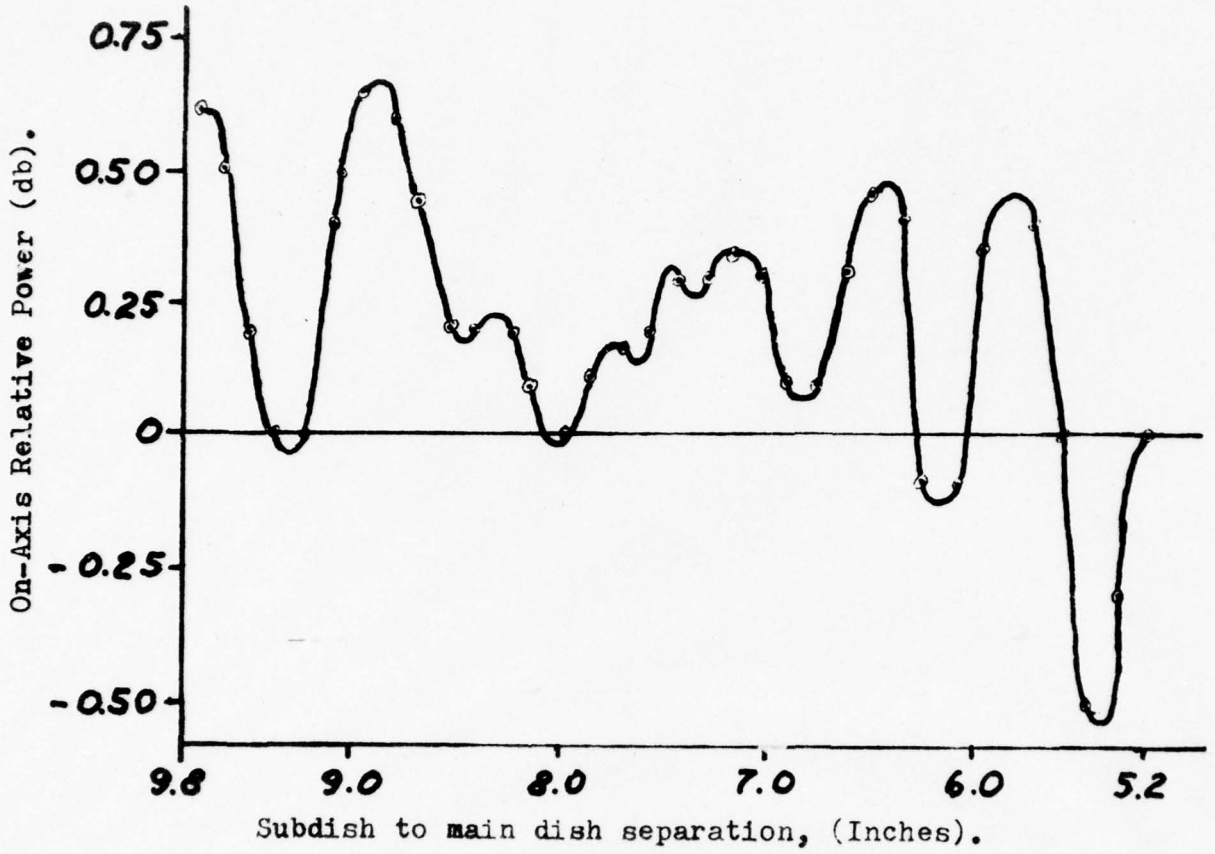

Fig. 3.8a. On-Axis relative power versus feed horn to main dish-85 feet.

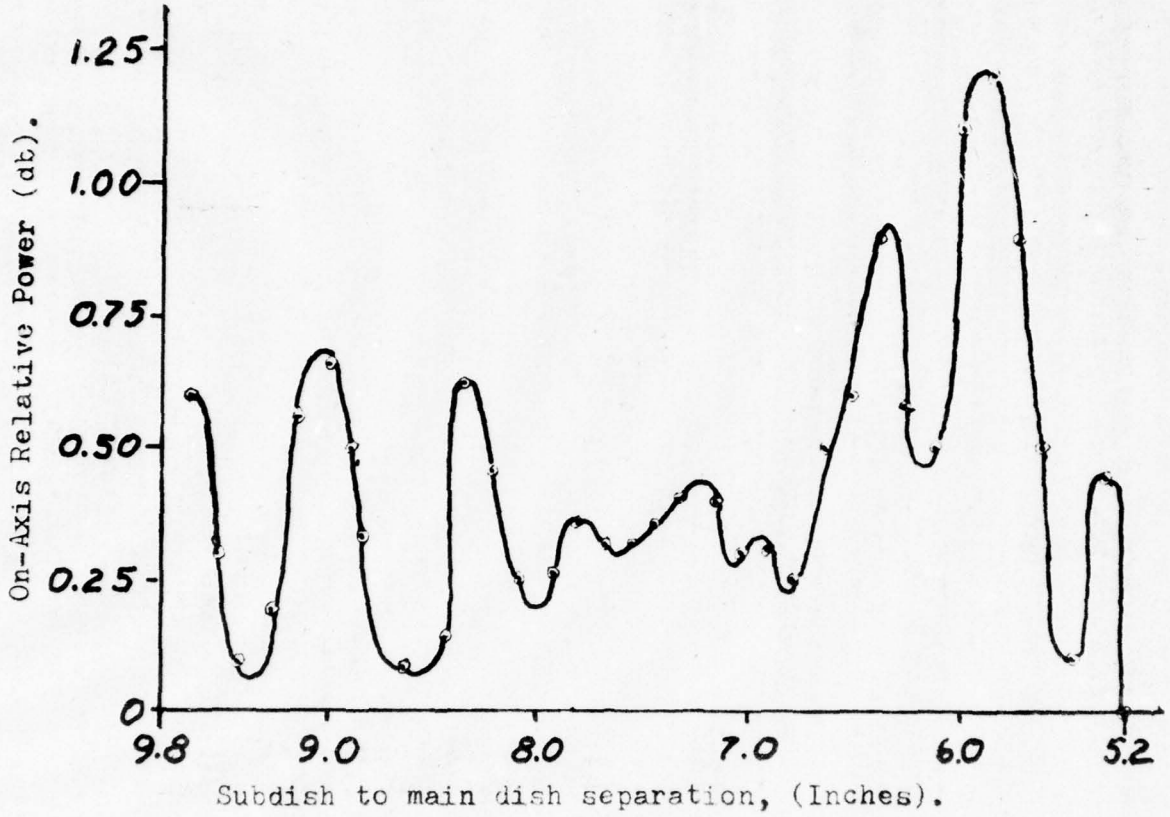

Fig. 3.8b. On-Axis relative power versus feed horn to main dish-35 feet.

where k is a constant related to efficiency. Since the efficiency of a well designed Cassegrain antenna is known to be 55%[3], k = 0.55 was used to find G_o. The values of these factors for the feed horn, the complete feed system, and the Cassegrain antenna operating at 9.197 GHz in each of the positions described previously are shown in Table 3.3 as are the factors for the Cassegrain operating at 9.275 GHz.

The decrease in beam area and corresponding increases in directivity, effective aperture and gain are readily apparent as the feed horn is brought closer to the subdish. It is also easily seen that the antenna performance improved when the operating frequency was changed.

The equation for directivity (Eq. 3.14) shown above is specifically derived for use with an antenna with a small beam area. The error for a case where the beam widths are both 75.2^o is ten percent. The directivities shown for the feed horn and feed systems in Table 3.3 are accurate to within ten percent, and are suitable for comparison purposes.

It is possible to estimate the maximum bandwidth of the feed horn-subdish, functioning as a spatial filter[2]. Assume that a frequency, f_c, for which an integral number of half-wavelengths exactly fits in the interval between the feed horn and the subdish, and designate f_o as the "original

	B_m (No Units)	D (No Units)	A_e in^2	G (db)
Feed Horn	1368	30.16	3.99	12.20
Feed System, Horn:				
Design Position	1365	30.22	4.00	12.21
2¼" Forward	1122	36.77	4.87	13.06
4¼" Forward	832	49.58	6.57	14.36
Cassegrain Antenna, Horn:				
Design Position	9.4980	4343.34	575.17	33.78
2¼" Forward	9.1860	4490.86	594.70	33.93
4¼" Forward	7.1356	5981.30	765.59	35.02
Cassegrain (9.275 GHz), Horn:				
Design Position	4.22	9770.45	1258.30	37.30

Table 3.3. Performance Factors

frequency" for comparison purposes. If we associate the original frequency with its free space wavelength (λ_o), then:

$$\lambda_o = \frac{c}{f_o} \quad , \tag{3.18}$$

where c is the free-space velocity of light. If the spacing between the horn and the subdish is increased by one-quarter wavelength ($\lambda_o/4$), then the resonator will resonate at a frequency (f_{new}), with a corresponding wavelength (λ_{new}),

$$f_{new} = \frac{c}{\lambda_{new}} = \frac{4}{5} f_o \tag{3.19}$$

and

$$\lambda_{new} = (\lambda_o + \lambda_o/4) = \frac{5}{4} \lambda_o . \tag{3.20}$$

Similar reasoning applies to the case in which the spacing between the feed horn and the subdish is decreased by $\lambda_o/4$ which results in:

$$\lambda'_{new} = (\lambda_o - \lambda/4) = \frac{3}{4} \lambda_o \tag{3.21}$$

and

$$f'_{new} = \frac{4}{3} f_o \tag{3.22}$$

The range of the spatial filter then, is from $f_{new} < f_o < f'_{new}$. It should be noted that f_o is not the

arithmetic mean of the range. It is significant that the total distance covered by $\lambda/2$ is on the order 1.5 cm (0.6") in the frequency range of the antenna designed for this study.

If f_o were 9.197 GHz, substitution into Eq.(3.20) and (3.22) above would yield

$$f_{new} = 7.35 \text{ GHz} \tag{3.23}$$

and

$$f'_{new} = 12.29 \text{ GHz} \tag{3.24}$$

or a bandwidth for the spatial filter of 4.94 GHz, which is the change in frequency needed to move from one minima of the curve in Fig. 3.3 to the adjacent minima.

E. Laser Excitation

In the course of antenna design using ray optics approximations, it was concluded that it should be possible to verify the design by exciting the antenna with a light source. The limitation of such an approximation of a microwave due to the extremely short wavelength of light was recognized, but it was further concluded that since the D/λ ratio would be very large, blockage effects would be negligible.

Initial attempts to excite the antenna with an incoherent light source were only partially successful. A small incandescent bulb was placed inside the feed horn, which was covered with black tape with a pin hole in the center to approximate a point source. This method produced main dish illumination on the order of 50%, and a high degree of light leakage.

The feed horn was then removed and a Laser beam fed through a prism was used as a feed system. This feed system improved the illumination to some degree, but more importantly, produced an intense illumination, and clearly indicated axial symmetry errors. It is doubtful that this lack of axial symmetry would have been discovered in any other manner.

Cross hairs were then mounted across the aperture in the path of the beam, and the axial symmetry of the system was corrected. A beam expander was then introduced in an attempt to illuminate a greater portion of the subdish, and hence, the main dish. As a result of space limitations, the maximum illumination obtained was on the order of 90% of the main dish (Fig. 3.9a). Since the surface of the main dish was highly polished and approached mirror smoothness, light was reflected from the parabolic main dish, and appeared on a wall several feet in front of the antenna. The illumina-

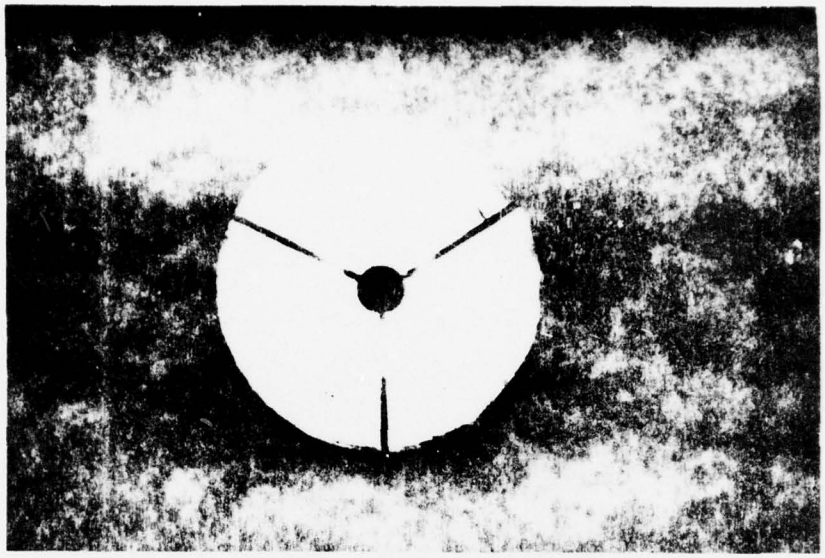

Fig. 3.9a. Cassegrain Antenna excited by Helium Neon Laser, approximately 90% illumination.

Fig.3.9b. Projection of light from Fig. 3.9a.

tion of the wall was circular as would be expected, and contained a shadow of the subdish with illumination in the center of the shadow (Fig. 3.9b). Hannan[3] points out that as D_m/λ becomes large, blockage becomes negligible. Klein[14] describes Fresnel diffraction by a circular obstacle, and shows that illumination in the center of the shadow is a predictable phenomenon.

It was determined, however, that Laser excitation of the system can be a valuable design aid if applied before the antenna is mounted to avoid spatial limitations. The verification of axial symmetry can be carried out quickly and easily, and with sufficient equipment, the subdish could be fully illuminated, thereby making examination of main dish illumination possible.

CHAPTER IV. CONCLUSIONS AND RECOMMENDATIONS

A. Conclusions

The following specific experimental observations have been confirmed in this thesis:

1. The Cassegrain antenna is made up of multiple reflection systems whose on-axis dimensions are capable of constructively interferring with some waves, and destructively interferring with other waves, as shown in Chapter III, Sections C and D.

2. The radiation pattern of the primary feed is a critical function of its location with respect to the parabolic reflector, as shown by detailed measurements. Therefore, it is impossible to properly design a Cassegrain antenna, e.g., for minimum blockage or forward spillover, without detailed knowledge of the actual primary feed pattern to which the subdish is exposed within the Cassegrain configuration. The implications of this finding are that the aperture illumination and aperture taper are critically dependent upon the feed horn to subdish location. Thus, both the effective aperture and the gain of the Cassegrain are capable of undergoing significant changes when the feed horn is slid along the axis.

3. The possibility of multipath and its influence upon the on-axis oscillations may be excluded from the present discussion since reasonable evaluation of its possible effects show no multipath or an influence on the order of four times that measured, which implies that the multipath does not exist.

There is nothing in the findings presented herein which tend to refute the fact that both horn to subdish resonator effects and changes in aperture illumination with movement of the horn along the axis are the most important consequences.

If these findings are further confirmed by the swept measurement frequency measurement technique described in the next section, then every Cassegrain antenna should, in principle, be calibrated so that the influence of frequency changes can be accurately predicted.

B. Recommendations for Further Research

Further research should be conducted so that the Cassegrain antenna can be calibrated. The system elements should be fixed in their respective design positions, and a leveled frequency swept measurement performed.

This requires a receiver whose amplitude and phase characteristics over the frequency range of the transmitter are known precisely, and a broad band receiving antenna. That is, an antenna in which the gain, directivity and driving point impedance do not charge significantly over the frequency range. The effective aperture change will be calculated.

The amplitude variation and the phase change of the signal introduced by the horn to subdish resonator must be measured as the frequency is swept. Using the data so collected, an "error curve" can be produced, which may be used to predict antenna performance.

It is further recommended that the standing waves in the feed horn-subdish region be measured using a small dipole probe as shown in Fig. 4.1. Care must be taken that the probe apparatus remains entirely in the blockage shadow of the subdish. The introduction of the probe will perturb the field to some extent. This perturbation can be measured by the use of a second probe forward of the antenna for comparison purposes.

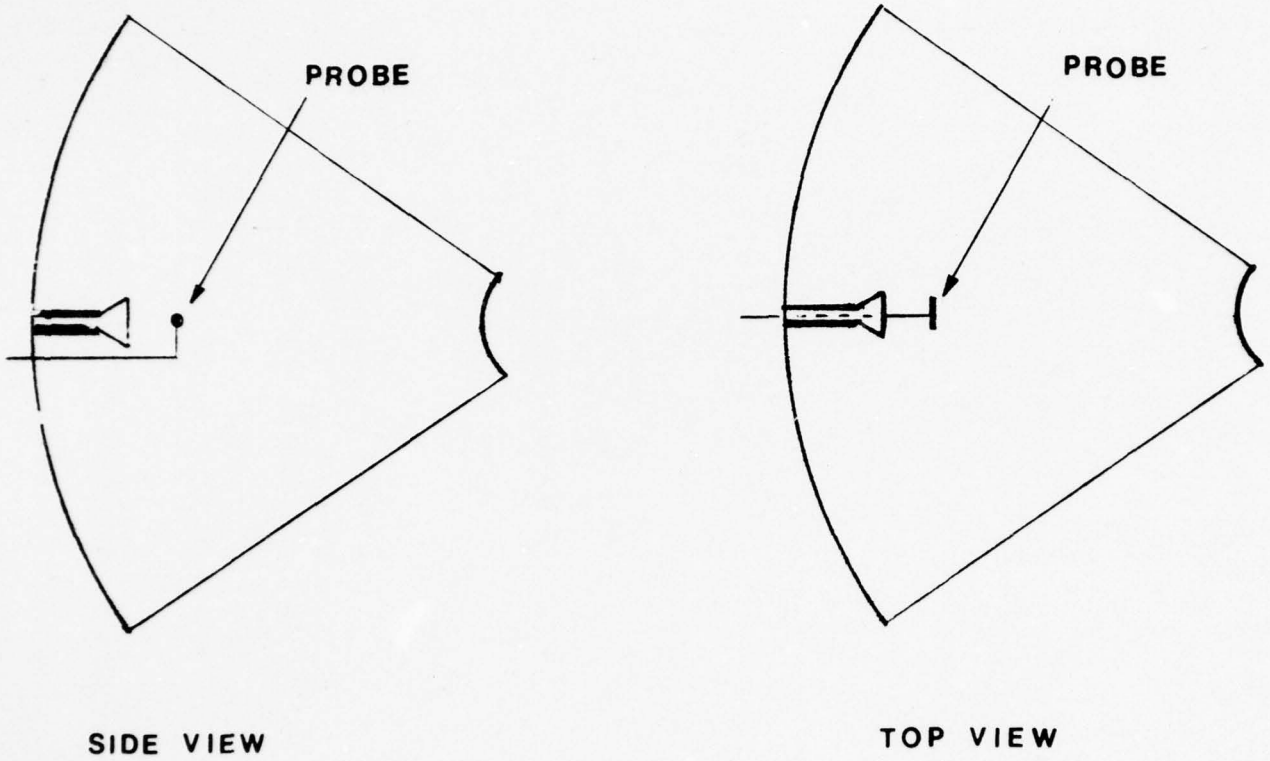

Fig. 4.1. Experimental Set-up using Dipole Probe.

REFERENCES

1. Bushko, G., B.S.E.E. Senior Project on The Characteristics of Cassegrain Antennas Employed in Radio Astronomy, F.I.T., 1973.

2. Nunn, W. M. Jr. and W. E. Claassen Jr., "Frequency-Dependent Effects in Cassegrain Antennas," Proc. 1975 IEEE Southeastcon, Charlotte, N.C., April 1975.

3. Hannan, P. W., "Microwave Antennas Derived From the Cassegrain Telescope," IRE Trans-PTGAP, No. 2, March 1961, pp. 140-153.

4. Jensen, P. A., "Designing Cassegrain Antennas," Microwaves, Vol. 1, No. 12, December 1962, pp. 12-21.

5. Henry, E. F., "Speed Design of Cassegrain Antennas," Microwaves, Vol. 9, No. 7, July 1970, pp. 46-48.

6. Cook, J. S., E. M. Elan and H. Zucker, "The Open Cassegrain Antenna: Part I - Electromagnetic Design and Analysis," Bell System Technical Journal, Vol. 44, No. 7, September 1965, pp. 1255-1300.

7. Zucker, H. and W. H. Ierley, "Computer-Aided Analysis of Cassegrain Antennas," Bell System Technical Journal, July-August 1962, pp. 897-932.

8. Selby, S. M., Standard Mathematical Tables, The Chemical Rubber Company, Cleveland, 1973, p. 372.

9. Kraus, J. D., Antennas, McGraw-Hill Book Company, New York, 1950, pp. 444-457.

10. Skolnik, M. I., Introduction to Radar Systems, McGraw-Hill Book Company, New York, 1962, pp. 282-286.

11. Kraus, op. cit., pp. 24-47.

12. Silver, S. (Ed.), Microwave Antenna Theory and Design, McGraw-Hill Book Company, New York, 1949, pp. 574-578.

13. Ibid., pp. 587-592.

14. Klein, M. V., Optics, John Wiley & Sons, Inc., New York, 1970, pp. 207-209.

15. Ibid., pp. 381-382.

REFERENCES NOT CITED

Burrows, M. L. and L. J. Ricardi, "Aperture Feed for a Spherical Reflector," IEEE Trans-PGAP, AP-15, No. 6, November 1967, pp. 227-230.

Dijk, J., C. T. W. van Diepenbeck, E. J. Maanders and L. F. G. Thurlings, "Efficiency and Radiation Patterns of Mismatched Shaped Cassegrain Antenna Systems," IEEE Trans-PGAP, AP-20, No. 5, September 1972, pp. 653-655.

Galindo, V., "Design of Dual-Reflector Antenna with Arbitrary Phase and Amplitude Distributions," IEEE Trans-PGAP, AP-12, No. 7, July 1964, pp. 403-408.

Green, K. A., "Modified Cassegrain Antenna for Arbitrary Aperture Illumination," IEEE Trans-PGAP, AP-11, No. 5, September 1963, pp. 589-590.

Halliday, D. and R. Resnick, Physics I and II, John Wiley & Sons, Inc., New York, 1966.

Jackson, J. D., Classical Electrodynamics, John Wiley & Sons, New York, 1962.

Jasik, H. (Ed.), Antenna Engineering Handbook, McGraw-Hill Book Company, New York, 1961.

Lorrain, P. and D. R. Corson, Electromagnetic Fields and Waves, W. H. Freeman and Company, San Francisco, 1962.

Morgan, S. P., "Some Examples of Generalized Cassegrain and Gregorian Antennas," IEEE Trans-PGAP, AP-12, No. 6, June 1964, pp. 685-691.

Potter, P. D., "Unique Feed System Improves Space Antennas," Electronics, Vol. 35, June 22, 1962, pp. 36-40.

Potter, P. D., "A New Horn Antenna with Suppressed Sidelobes and Equal Beamwidths," Microwave Journal, Vol. VI, No. 6, 1963, pp. 71-78.

Ramo, S., J. R. Whinnery and T. van Duzer, Fields and Waves in Communication Electronics, John Wiley & Sons, New York, 1965.

Rao, B. L. J. and S. N. C. Chen, "Illumination Efficiency of a Shaped Cassegrain System," IEEE Trans-PTGAP, AP-18, No. 3, May 1970, pp. 411-412.

Rudge, A. W. and D. E. N. Davies, "Electronically Controllable Primary Feed for Profile Error Compensation of Large Parabolic Reflectors," Proc. IEE (London), Vol. 117, No. 2, February 1970, pp. 351-358.

Rudge, A. W. and M. J. Withers, "Design of Flared-Horn Primary Feeds for Parabolic Reflector Antennas," Proc. IEE (London), Vol. 117, No. 9, September 1970, pp. 1741-1749.

Rusch, W. V. T., "Scattering from a Hyperboloidal Reflector in a Cassegrain Feed System," IEEE Trans-PGAP, AP-11, No. 7, July 1963, pp. 414-421.

Skolnik, M. (Ed.), Radar Handbook, McGraw-Hill Book Company, New York, 1970.

Stratton, J. A., Electromagnetic Theory, McGraw-Hill Book Company, New York, 1941.

Truman, W. M. and C. G. Balanis, "Optimum Design of Horn Feeds for Reflector Antennas," IEEE Trans-PTGAP, AP-22, No. 4, July 1974, pp. 585-586.

Viggh, M., "Designing for Desired Aperture Illumination in Cassegrain Antennas," IEEE Trans-PGAP, AP-11, No. 2, March 1963, pp. 198-199.

Williams, W. F., "High Efficiency Antenna Reflector," Microwave Journal, July 1965, pp. 79-81.


LMED
78